4.2 *The Platinotron: Amplitron and Stabilotron*

by W. C. BROWN

I. Introduction

The platinotron* resembles the magnetron, but differs from it structurally in that the rf circuit is non re-entrant and nonresonant, and requires two rather than one external rf terminations. The platinotron possesses directional properties. That is, if rf energy is fed into the input termination of the tube, it appears amplified at the output termination. In the reverse direction, no gain results and neither is there significant insertion loss in transmission of the impressed rf energy at the input termination. The operating frequency of the device is determined by external influences such as an injected rf signal, reflections from a mismatched transmission line, or reflections from a high-Q cavity.

The platinotron may be used as a compact, highly efficient nonlinear or saturated amplifier with nominal bandwidth and nominal power gain.

* The platinotron device is proprietary to the Raytheon Company. The experimental data reported here were obtained under a U.S. Signal Corps contract.

Typical efficiencies lie between 50 and 80%, bandwidth is about 10%, and gain is from 5 to 20 db, depending on rf drive. It is capable of handling very high peak or average power levels and unusually long pulse durations. In this role, the platinotron is referred to as the "Amplitron." * Its negligible "gauss line discontinuity effects" and low phase pushing (i.e., a tenth of that of other high power amplifiers, or of the order of 0.5 deg per 1% anode current change) means that power supply regulation and modulator pulse shape are not critical factors in its performance. Finally, by virtue of the directional and low insertion loss properties of the Amplitron, it is possible to low-level duplex on its input side. The Amplitron, however, is subject to interpulse oscillation which requires plate modulation to suppress it. Also, its terminations must be well matched for best performance.

Suitable feedback (i.e., reflection or mismatch in the output circuit) and stabilizing (i.e., high-Q cavity) components enable the platinotron to be used as a frequency stabilized self-excited oscillator operating with high stability, efficiency, and power output. When used in this capacity, the platinotron, together with its external components, is called a "Stabilotron." * It is capable of being simultaneously tuned and stabilized by a single cavity. In this mode of operation, part of the signal that is amplified through the platinotron is reflected by the feedback mismatch in the output circuit and travels through the platinotron back to the stabilizing system. This system in turn re-reflects only the energy that is at the resonant frequency of the stabilizing cavity and absorbs the energy that is not at the resonant frequency of the cavity. Thus the Stabilotron will oscillate only at the frequency of the high-Q tunable cavity. For a given degree of frequency stability, higher circuit efficiency can be realized in the Stabilotron than in a magnetron, since the stabilizing cavity can be placed at the input to the Stabilotron and hence absorbs less power; as a consequence, the over-all efficiency of the Stabilotron invariably falls between 45 and 60%.

The Stabilotron has such great operating stability that it removes many of the objections to using a self-excited oscillator as the source of the transmitted power in high quality radar systems. Contributing to this great frequency stability are the low frequency pushing figures (about one kilocycle per second per each percent change in anode current), the low pulling figure (about 0.5 Mc/sec at S-band) and the low starting time jitter (typically 2 mμsec at L-band).

Although the early applications of the Amplitron and Stabilotron have been in pulsed applications, there are no reasons why platinotron devices are not ideally suited for CW applications of both high power and low

* Raytheon trademark.

power variety. The same qualities that make for a highly stable pulsed Stabilotron also make for a highly stable low power oscillator of the local oscillator type. The CW Amplitron is ideally suited for high power applications, but its nominal gain limitations prevent it from being of great importance for low power applications.

Because of its close similarity to the magnetron in construction, it is surprising that the platinotron or a similar continuous-cathode amplifier device has been so tardy in coming into being. It was well-known, for example, that the magnetron had a very broad-band circuit and that the circuit re-entrancy was the cause of the narrow band of the device. There was indeed some modest effort expended in an attempt to make a more versatile operating device out of the conventional magnetron (*1*). The failure of a greater effort to develop was probably caused by both the formidable analytical problems which made the magnetron approach unattractive to many investigators, and the publishing of attractive performance characteristics from an amplifier device (*2*) much more amenable to analyses. Another possible reason for the failure of the magnetron approach to mature earlier was the failure on the part of engineers to recognize that there were important applications for a saturated amplifier of broad-band properties, quite independent of whether that device also had linear amplifier characteristics. The final emergence of the platinotron device, then, is partly the result of a persistence in forsaken fields and partly the result of a critical review of what performance characteristics in a microwave tube were really fundamental and essential to equipment applications.

The emergence of the platinotron may have significance other than its immediate usefulness as a broad-band amplifier and stable oscillator; it may help support a revival of interest in the crossed-field device viewed in a more general sense.

II. The Amplitron

A. Physical Description

Figure 1 shows a typical platinotron, the QK434, with the external magnet and cover removed, exposing the internal circuit and cathode. Physically the device is similar to the conventional fixed frequency magnetron oscillator. Like the magnetron, the electron beam is re-entrant and originates from a continuously coated cathode which is coaxial to the rf circuit. Like the magnetron, the device is placed in operation by supplying a static magnetic field parallel to the axis of the cathode and an electric potential between the cathode and the rf circuit. But unlike the

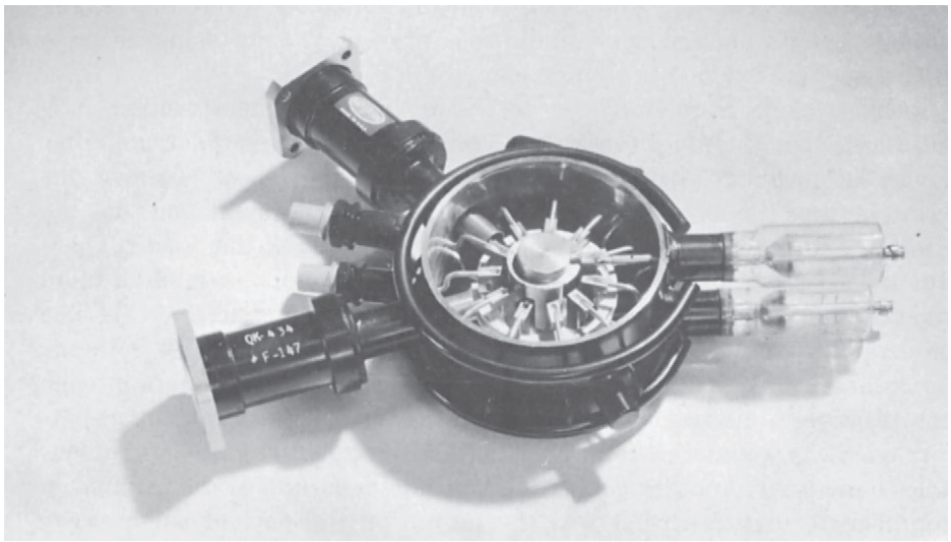

FIG. 1. Photograph of a platinotron with the magnet and one cover removed.

conventional magnetron oscillator, the rf circuit is non re-entrant* and the characteristic impedance of the rf circuit is matched at both ends of the circuit to two external rf connections over the frequency region of interest. This difference in the treatment of the rf circuit results in completely different operating behavior of the conventional magnetron oscillator and platinotron. The platinotron circuit treatment not only provides the two sets of terminals necessary for an amplifier, but it takes advantage of the natural broad-band characteristics of the rf circuit which the re-entrant circuit treatment in the magnetron nullifies.

As shown in Fig. 2, the rotation of the space-charge cloud may be in either direction in the conventional magnetron oscillator without causing noticeable differences in performance, whereas in the platinotron, changing the direction of rotation relative to the input and output of the device will bring about a radical change in the behavior of the device.

Additional perspective as to the physical nature of the device may be obtained from Fig. 3 which gives salient views of a typical platinotron.

B. Characteristics of the Device as a Circuit Element

As a circuit element the platinotron may be described as an active two-terminal-pair network with directional properties, as shown in Fig. 4.

* The cutting of the straps of a strapped platinotron circuit provides a high degree of isolation between the two circuit members thus formed.

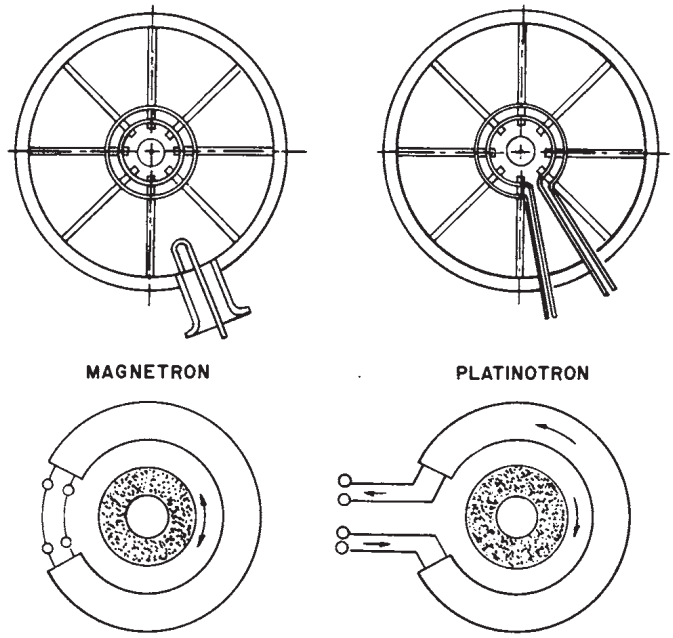

FIG. 2. Diagram illustrating the basic differences of construction and operation between the platinotron and the magnetron.

When an rf signal is injected into the first set of terminals, the rf level will be greatly increased at the second set of terminals. On the other hand, if the rf signal is injected into the second set of terminals, the rf level will be neither increased nor decreased at the first set of terminals. To a first approximation, there will be the same phase shift θ_p of the rf signal as it traverses the device, regardless of direction. If the direction of the magnetic field is reversed, then the directional properties of the device are also reversed.*

Various performance characteristics of the device based on this simplified circuit concept can now be discussed. The first characteristic to be discussed is the relationship between rf input and rf output as a function of dc power input to the device. These characteristics for a platinotron (Raytheon QK434) are shown in Fig. 5. Quite clearly, the device behaves as a saturated amplifier. For a given dc power input level, the rf output is relatively independent of the rf drive level, departing from

* The directional properties of the device may also depend upon the current level at which the device is operated. At very low current levels the QK434 has been found to have a forward wave type of interaction, but at the current levels at which the QK434 would be operated as a power device, the beam circuit interaction is of the backward wave type. The shift occurs at a value of anode current from two to three amperes.

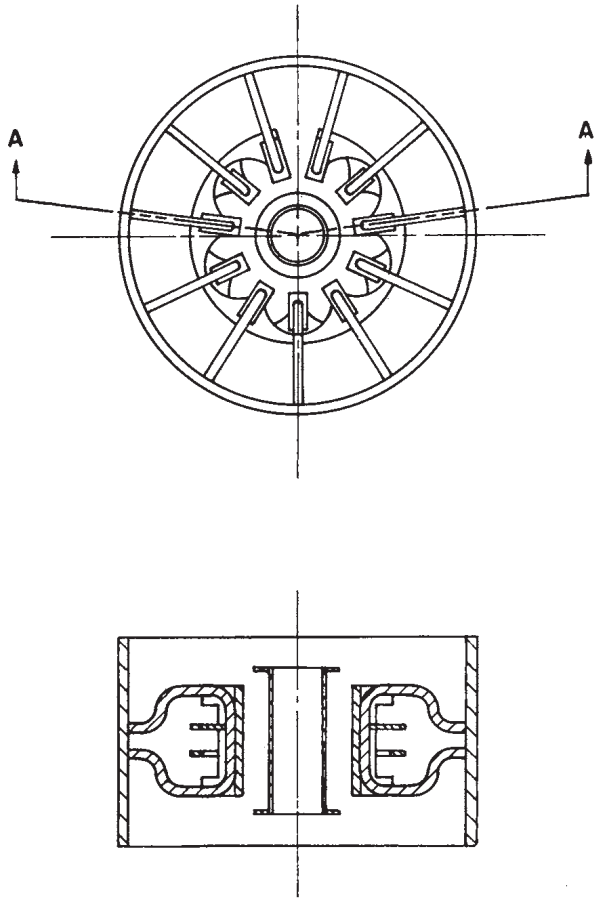

FIG. 3. Plan and cross section view of an L-band platinotron.

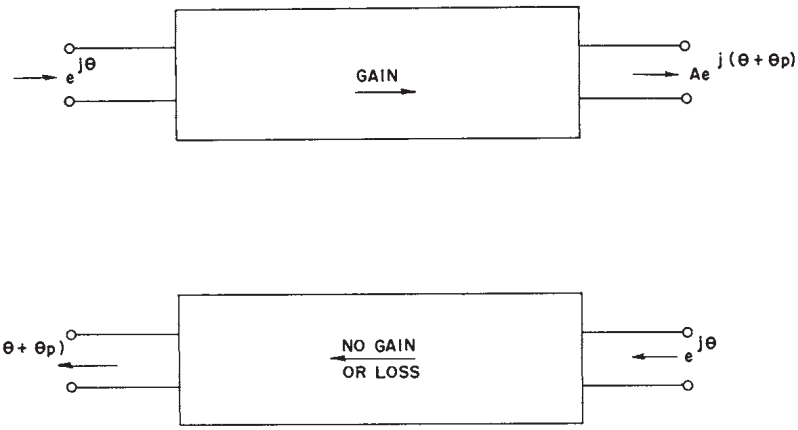

FIG. 4. The circuit element characterization of the platinotron.

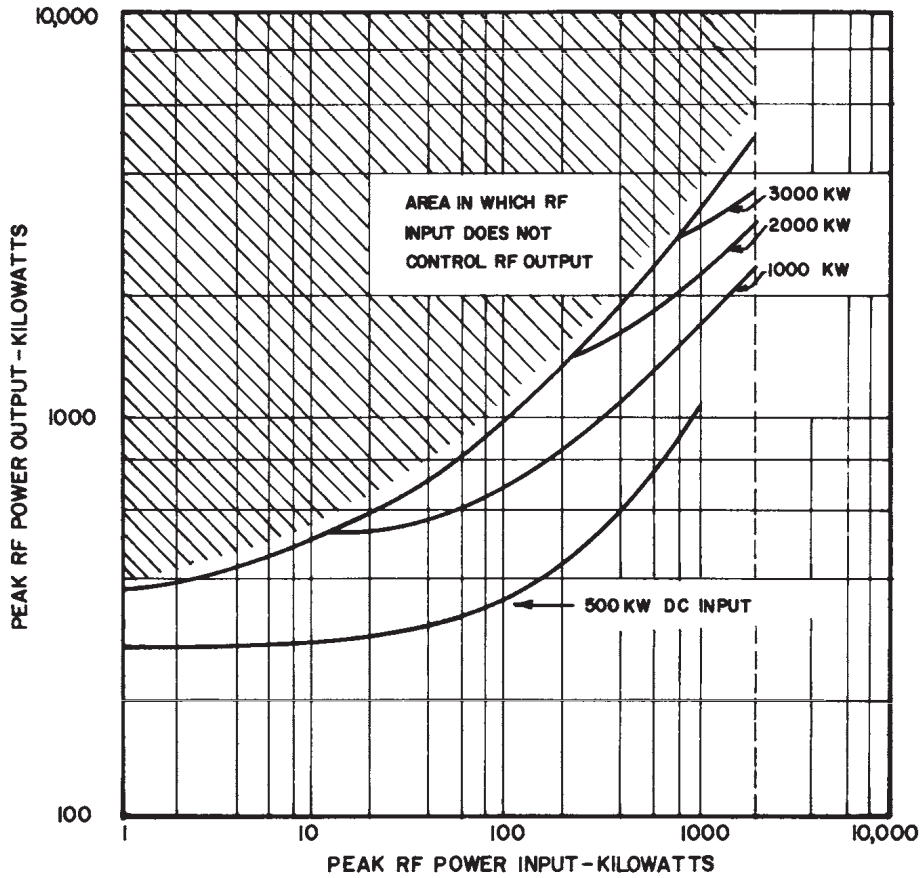

FIG. 5. The general relationship between the rf input and the rf output of the QK434 platinotron as a function of pulsed power input from the modulator.

this independence as the magnitude of the rf drive level becomes comparable to the rf output level, and as the rf drive level becomes so low that it loses control over the frequency of the rf output. In the region in which the rf input does not control the rf output, the rf output is noisy, poorly defined, and at some other frequency than the driving signal. The transition region between the controlled and uncontrolled areas is well defined and of negligible width.

The operation of this platinotron has been explored with rf drive levels as low as 2 kw to as high as 2000 kw. Over this range of driving signal, the curve marking the separation of the controlled and uncontrolled regions of operation has been found to be approximately

$$P_{o'rf} = \frac{K^2}{4} + K\sqrt{P_{i'rf}} + P_{i'rf}$$

where

$$K = 43.2$$

$$P_{o}\text{rf} = \text{rf power output in kw}$$

$$P_{i}\text{rf} = \text{rf power input in kw}$$

This curve also determines the maximum gain that can be obtained at any rf drive level.

$$\text{Maximum gain} = \frac{P_{o}\text{rf}}{P_{i}\text{rf}}$$

$$= \frac{K^2}{4P_{i}\text{rf}} + \frac{K}{\sqrt{P_{i}\text{rf}}} + 1$$

As indicated in the above equation and Fig. 5, power gains of 20 db may be obtained at the lower drive levels, whereas gains of only a few db may be expected at the higher drive levels. It should be noted, however, that the rf input power is conserved in the rf output power, making it possible to use efficiently the higher power but lower gain levels of the platinotron.

The rf power which is generated within the platinotron flows predominantly out of the output set of terminals only. The fraction of the generated power which finds its way to the input set of terminals and appears at those terminals as reflected or reverse-directed power is only a small fraction of the output power of the device. This behavior is distinctly different from that associated with a conventionally locked oscillator. The ratio of the reverse-directed power to the output power for the QK434 is shown as a function of frequency in Fig. 6. If the reverse-directed power originates from a reflection at the output of the device, however, it passes back through the tube relatively unattenuated. The manner in which this device handles the power generated within it and the manner in which it handles reflected power from the output substantiates the circuit representation of Fig. 4.

A very interesting and useful property of this device is its ability to amplify, operate efficiently, and deliver large power output over a relatively wide frequency band. A typical plot of efficiency against frequency at a fixed power input level is shown in Fig. 7. The efficiency remains relatively constant over a 10 percent or greater frequency band.

Another characteristic of this device of considerable practical importance is that the phase shift across the device is nearly independent of the dc current applied to the device over a relatively wide range of currents. The term "phase pushing" has been applied to the slope of the characteristic of frequency vs current because of its relationship to the term "frequency pushing" which is descriptive of a similar phenomenon in oscillators in which the frequency is changed or "pushed" as the cur-

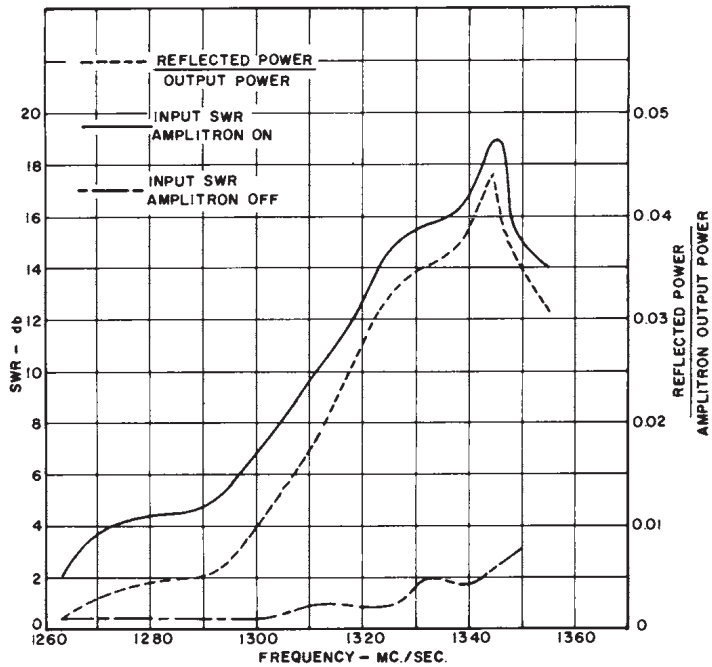

FIG. 6. Measurement of a reverse-directed power at the input of the platinotron as a function of frequency with the platinotron operating into a matched load.

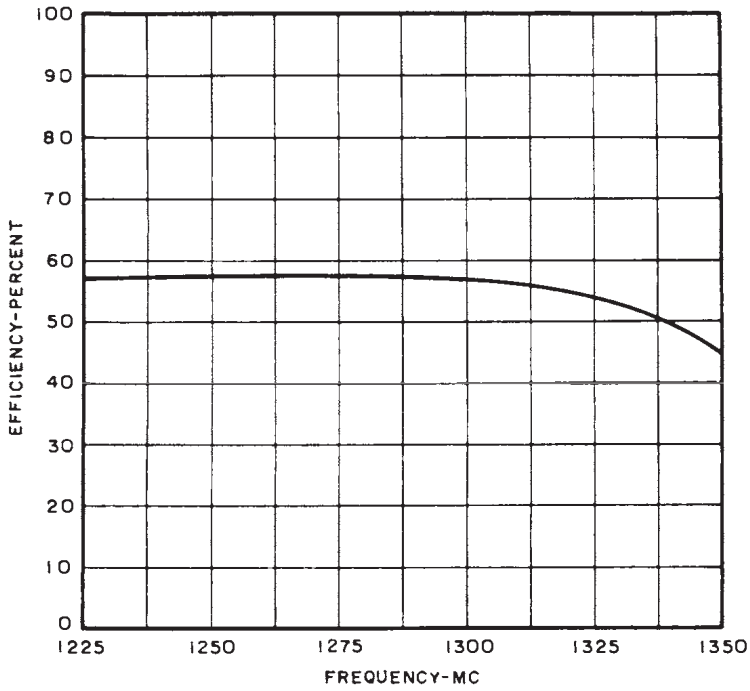

FIG. 7. Efficiency vs frequency relationship typical of platinotron performance.

rent is changed. In the platinotron device the phase pushing can be measured either directly by noting the change in phase across the device as the current is changed, or it may be measured indirectly by using the platinotron as an oscillator and measuring the frequency change. In conventional magnetron oscillators, the frequency pushing can change from a positive value to a negative value, going through a zero value, as the current is increased. Similarly, in the platinotron the "phase pushing" can obtain a value of zero. However, its value everywhere in the operating range is so low as to make quantitative measurements of phase pushing difficult. It has been necessary to note the phase change resulting from a relatively large change in current, and thereby obtain an average value of phase pushing over this current range. Table I has been prepared from such data. These data indicate that the phase pushing does go to zero and is everywhere small in value.

TABLE I

EXPERIMENTALLY MEASURED PHASE PUSHING CHARACTERISTICS IN AN L-BAND PLATINOTRON

kv	10–20 A	20–30 A	30–40 A
36	−0.8°/amp	+0.34°/amp	30–34A +0.85°/amp
34.6	−0.45°/amp	+0.22°/amp	30–34A +0.8°/amp
33.2	−0.44°/amp	+0.22°/amp	+0.9°/amp
30.3	−0.6°/amp	+0.40°/amp	+0.8°/amp
25.9	−0.8°/amp	+0.60°/amp	+0.9°/amp

Considerably better data have been obtained on phase pushing by measuring the frequency pushing when the platinotron device is set up as a self-excited oscillator, its frequency being primarily controlled by the relative position of reflections deliberately placed in the input and output. Such data are shown in Fig. 8 where it is clearly seen that the slope of the frequency vs current characteristic has a zero value for certain values of current and magnetic field. Since an oscillator in the steady state must always maintain a total loop phase shift of some integral multiple of 2π radians, and since the oscillator is composed of elements whose phase shift is dependent upon frequency, a constant frequency can only be obtained if the phase shift remains constant. If the frequency of such an oscillator remains constant as the current is varied,

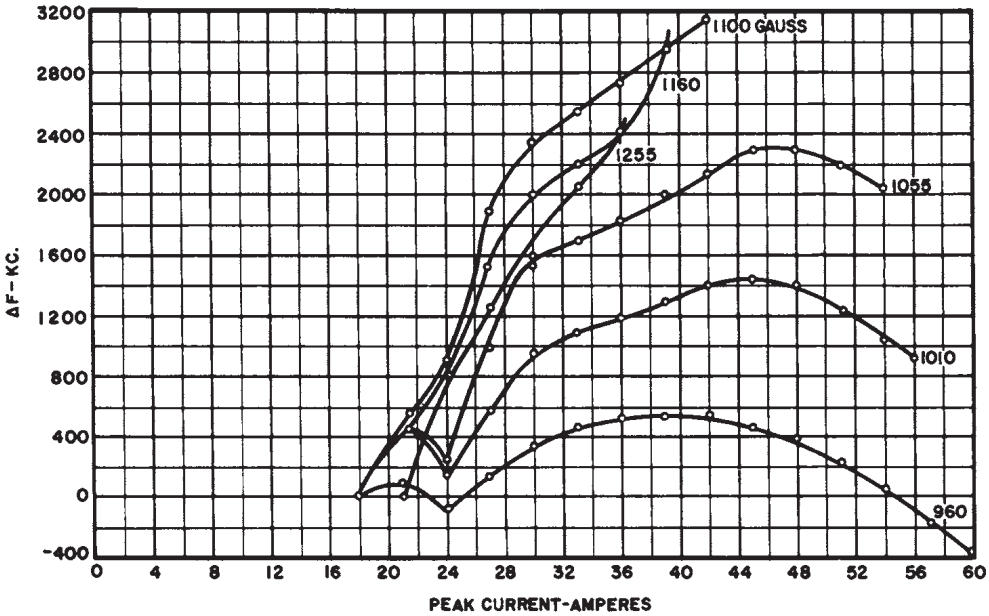

FIG. 8. Experimentally measured frequency pushing characteristics in an L-band platinotron operated as a nonstabilized oscillator.

the conclusion may be drawn that the phase shift also remains constant over the current region.

The possibility of obtaining zero or small phase pushing in an amplifier is of considerable significance in the design of many radar systems in which it is desired to hold the phase shift across the device constant while still making the modulator as simple and compact as possible.

The relationships between anode voltage, anode current, frequency, and magnetic field are of primary importance. These relationships are similar to those for a magnetron device, and will be developed later in this section. Representative data giving the relationship between anode voltage, anode current, and magnetic field, with the frequency held constant are shown in Fig. 9. The platinotron is a relatively low input impedance device, ranging from 500 to 1000 ohms depending upon the operating point which is selected.

C. Performance Characteristics

Although the platinotron device itself has been described as an amplifier, it is possible to use it as a self-excited oscillator, either stabilized or unstabilized. The term "Amplitron" has been assigned to the use of a platinotron in those applications where it is intended to drive it with an rf signal. The following material therefore describes the characteristics

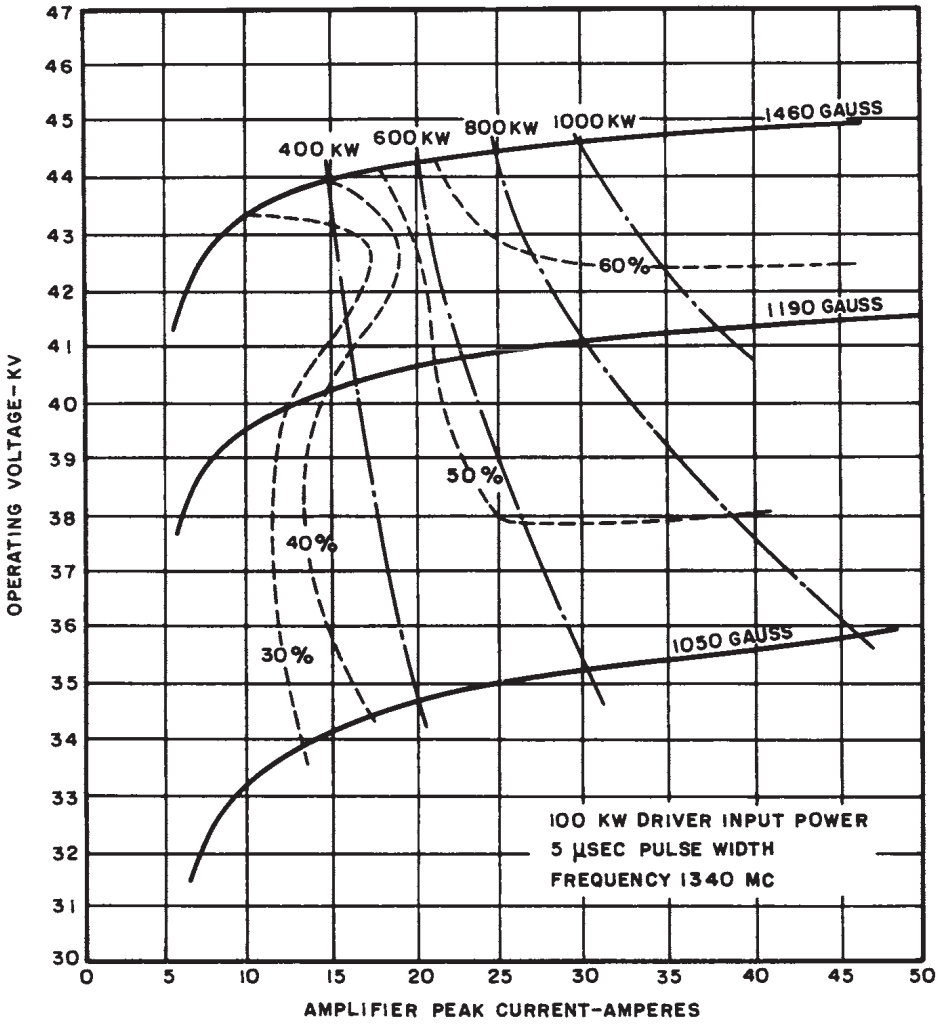

FIG. 9. Typical performance chart of an L-band platinotron (QK434). Curves of constant rf power output and efficiency are shown.

of the platinotron when it is used as an amplifier, and the term Amplitron will therefore be used.

In evaluating the performance of an amplifier, there is a natural major concern as to the quality of the reproduction of the input signal. From the standpoint of evaluating the quality of reproduction, the usual ordinary measurements of efficiency, power output, gain, etc., are not sufficient. It is desirable to take each point of data in such a manner that a measure of the quality of the reproduction of the input signal is available. This is accomplished by photographing the input and output frequency spectra presented on a voltage basis on a spectrum analyzer. The voltage

spectra are particularly useful as critical measurements, for the spectrum sidelobe structure is very sensitive to any reproduction change. As a further enhancement of critical evaluation, a relatively long pulse duration of 5 μsec is used. This results in a spectrum bandwidth of 400 kc between the first null points of the spectrum.

For Amplitron tests, obtaining a good driver spectrum posed considerable difficulty. This problem was solved finally by using a Stabilotron as the driver. Because spectrum analyzers of sufficient resolving power and stability were not generally available, a special analyzer was developed for the purpose of taking spectral data.

The Amplitron tested was designated the QK520. Separate modulators for the driver and the Amplitron were used but the trigger of one was slaved to the other. The times of the start of the two pulses and the pulse widths were made as nearly identical as possible. In the rf circuit, a resistive pad was inserted between the driver and the Amplitron, primarily for the purpose of reducing the power output of the driver to a usable input signal level for the Amplitron. The pad served a second function in that it effectively isolated the driver from the Amplitron. Such isolation is of particular importance when the Amplitron is operated into a mismatched load.

The measurement of Amplitron efficiency requires definition and discussion. In a nominal gain device where the input power appears as an appreciable percentage of the output power, a conservative definition of efficiency must make provision for the subtraction of this input power from the output power. Consequently, in all the data presented the following conservative definition of efficiency is used:

$$\text{Amplitron efficiency} = \frac{\text{rf power output} - \text{rf power input}}{\text{modulator power input to Amplitron}} \tag{1}$$

The definition of Amplitron gain is, of course,

$$\text{Amplitron power gain} = \frac{\text{power output}}{\text{power input}} \tag{2}$$

Although the Amplitron efficiency should be defined as above, it should be remembered that the input power is not lost but appears as part of the output power. The effective over-all efficiency of a chain of Amplitrons can therefore remain very high.

In evaluating this device we must consider the effects of varying the parameters of anode voltage, anode current, magnetic field, level of rf drive, frequency of rf drive, and the load into which the tube operates. Over a very wide variation of these parameters the spectra reproduction should remain satisfactory throughout the region and not vary discontinuously in any manner. Therefore, the spectrum was photographed at frequent intervals of the parameters that were being varied.

D. Matched-Load Performance

These data are presented in the same manner in which magnetron data are often presented. The relationship between anode voltage and anode current is determined by the magnetic field strength, as indicated in Fig. 10 by the four "Gauss" lines. The reproduction of the input spectrum is indicated at 5 amp increments along each Gauss line. Over the region

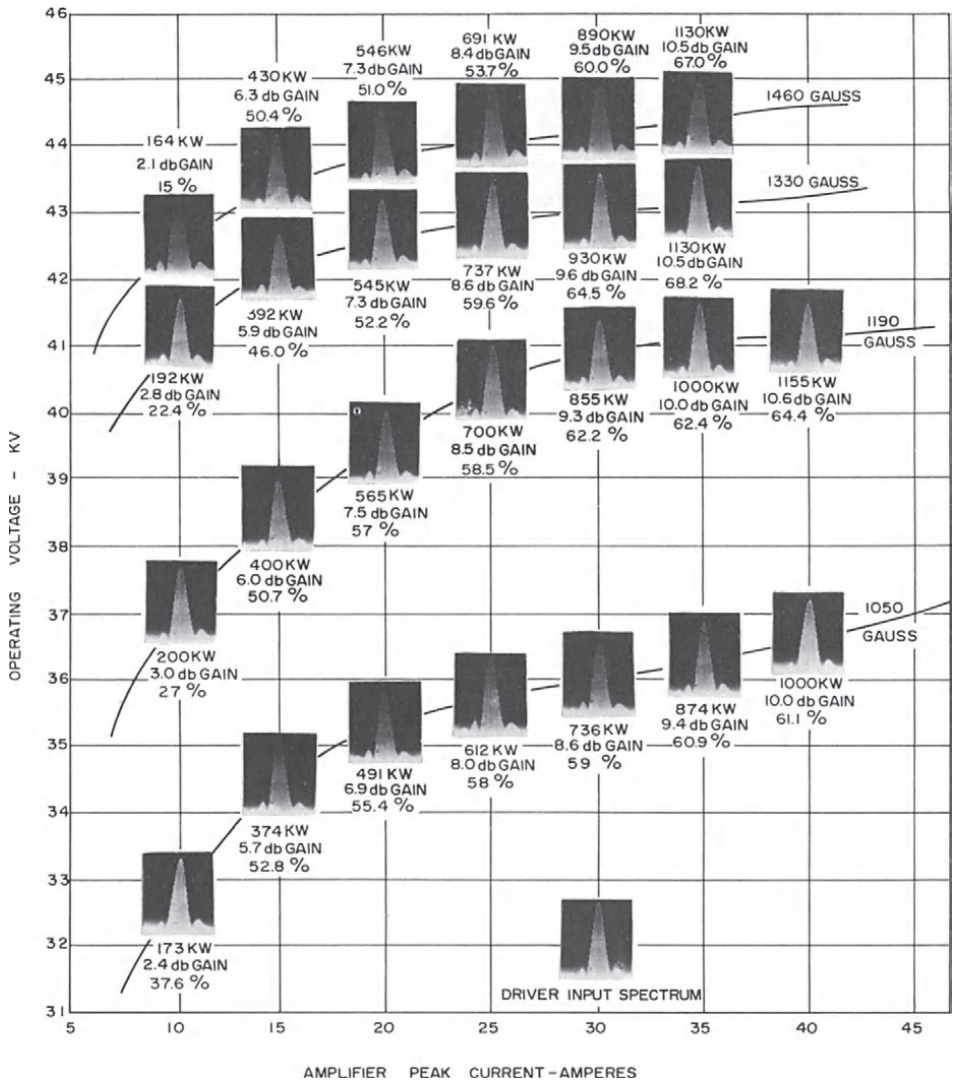

FIG. 10. Amplitron (QK520) matched-load performance with output spectra at a frequency of 1290 Mc and an rf drive level of 100 kw. Pulse width 5 μsec and duty 0.001.

of the graph in which spectra data are shown, the quality of the spectra is good and there are no regions of poor spectra. The highest current values for which spectra are shown mark the limits of amplification of the Amplitron and indicate that good spectrum quality is maintained as the upper current boundary is approached. If the upper current boundary is exceeded, there is complete failure of amplifier action.

Power output, efficiency, and gain are shown below each spectrum photograph. The particular data shown in Fig. 10 indicate increasing efficiency with increasing current and magnetic field. Efficiencies in the range of 60–65% are attained.

These particular data were taken with an rf input power of 100 kw. Similar data taken at 10 kw and 50 kw of rf drive indicate no discontinuities of spectra quality over wide variation of the parameters of magnetic field and current. With the higher drive power, higher peak powers as well as higher efficiencies are obtained, but the maximum value of gain is lower. With the lower values of drive power, the maximum gain values are as high as 16 db, but the maximum power output is greatly reduced. The increase in maximum gain and decrease in maximum power output with decreased rf input is characteristic of the QK520 L-band Amplitron discussed herein and is characteristic of Amplitrons in general.

The data discussed above were taken at 1290 Mc. Similar data were taken at 1240 and 1340 Mc and followed the same general pattern as those taken at 1290 Mc.

A somewhat more instructive way of presenting data for the operating conditions which the Amplitron will actually experience in service involves holding the magnetic field constant and examining the performance over a wide range of frequency and current. Figure 11 shows such data taken with an rf input of 90 kw. Spectrum photographs were taken at 5 amp increments of current and 25 Mc increments of frequency to cover a 10% frequency range. By means of these data it is possible to determine the gain level and efficiency with which it is possible to cover the 10% frequency band while keeping the current constant. It may be noted that the efficiency exceeded 50% at a 9.5 db gain level over most of the band. Similar data have been taken at lower rf drive levels. With a 10 kw drive level an amplification of 15.5 db with good reproduction over an 8% frequency band was obtained.

E. Variable-Load Performance

To be practical, an amplifier must be capable of operating into a mismatched load of arbitrary phase and standing wave ratio of at least 1.5

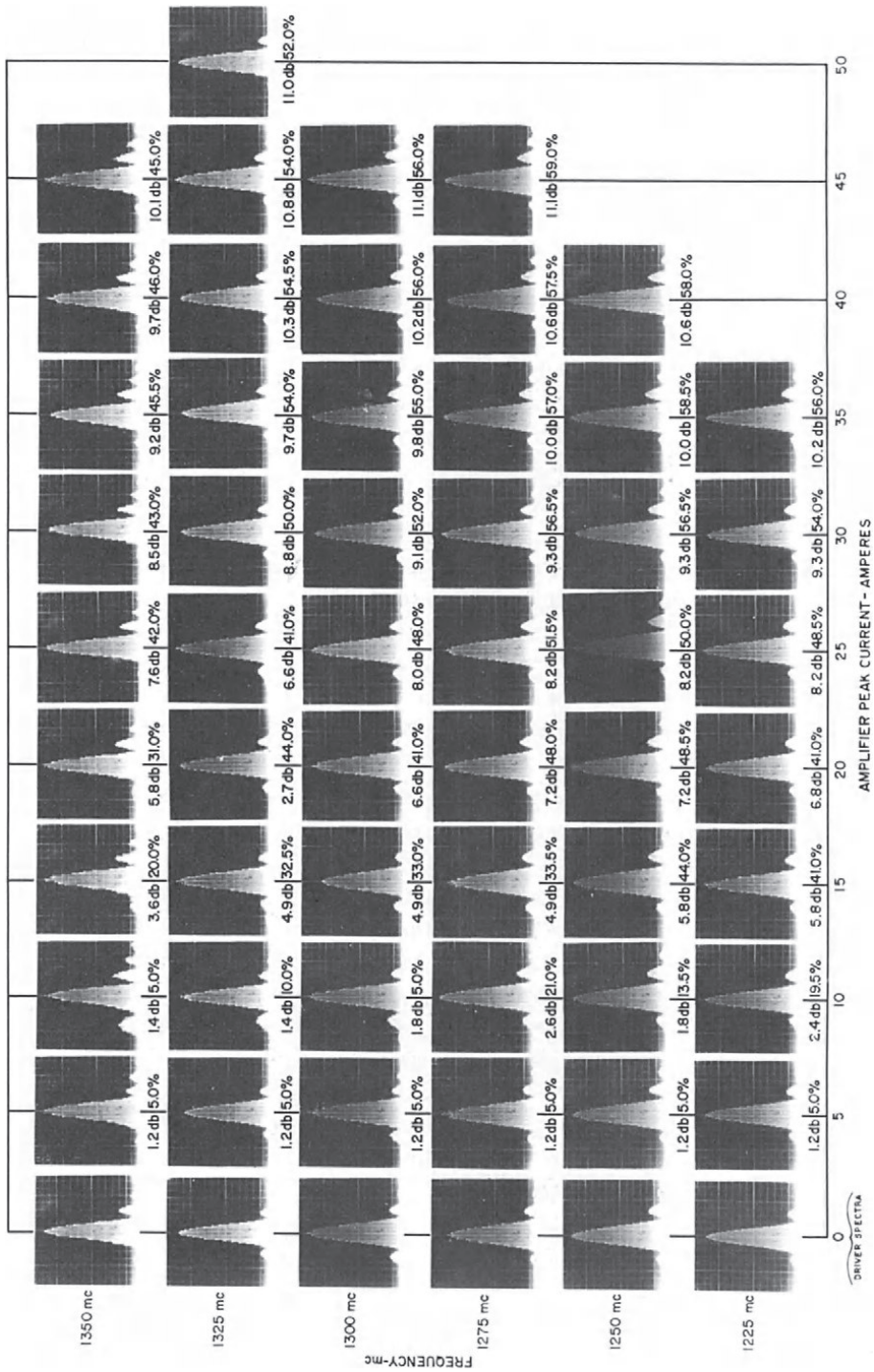

FIG. 11. Amplitron matched-load performance at an rf input level of 90 kw and with the magnetic field held constant. Pulse width 5 μsec and duty 0.001.

in voltage and preferably higher. To examine the ability of the Amplitron to meet these requirements, spectrum photographs and other essential data were taken for representative mismatches and plotted on load diagrams similar to that shown in Fig. 12. Spectra were taken for eight equally spaced phase positions of a 2.5/1 VSWR and 1.5/1 VSWR, and

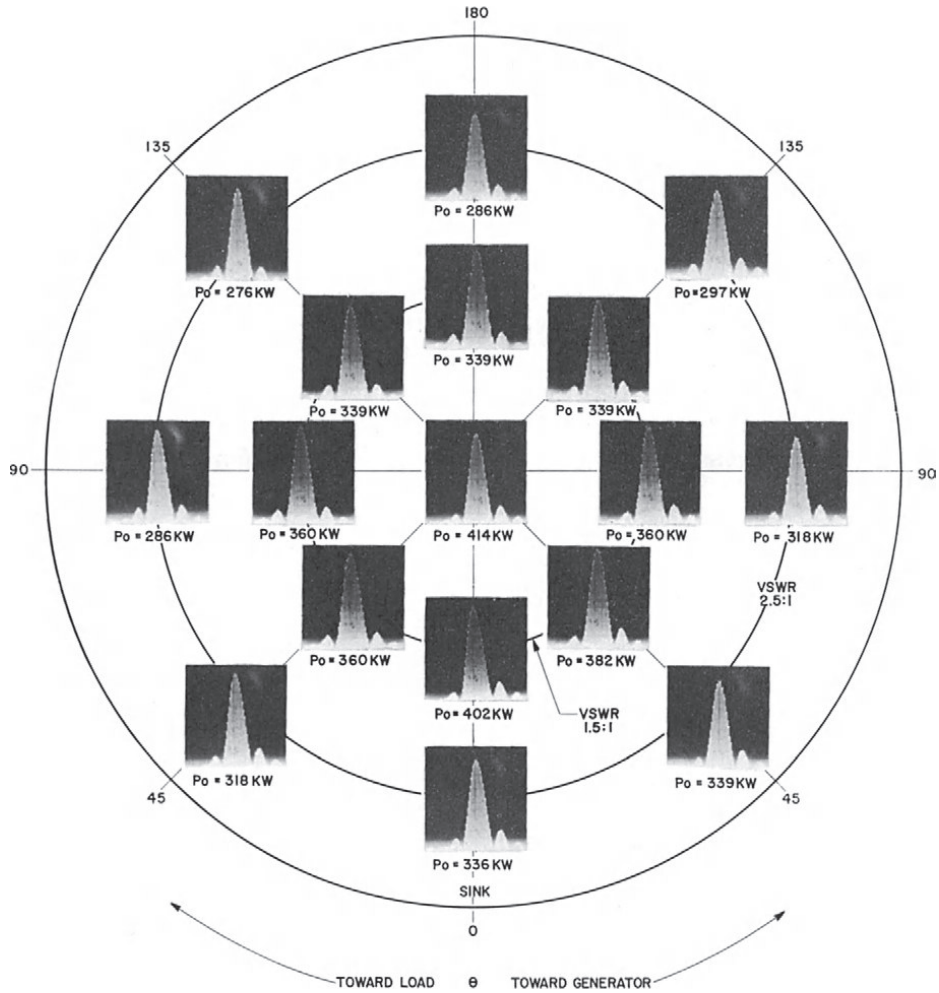

FIG. 12. Amplitron performance as a function of load at 1240 Mc and with an rf input level of 10 kw. Applied voltage 39 kv, average current 20 ma, duty 0.001, pulse width 5 μsec, driver isolation 12 db attenuator.

at the match point. The shape and quality of the spectrum varied a negligible amount under these varying conditions of load. The data of Fig. 12 are particularly interesting since the drive power of only 10 kw permits a gain of 16 db at the match point. The reflected power from a 2.5/1 VSWR therefore represents a reflected power of over seven times the

input power. The bulk of this reflected power is absorbed in the input pad between the driver and the Amplitron. The data are of further interest in that they were taken at 1240 Mc which is very near one frequency edge of the band. Similar data have been taken at 1290 Mc and 1340 Mc, respectively.

The fact that all the input power appears in the output power of the Amplitron, and is therefore not wasted, gives rise to consideration of the use of Amplitrons at relatively low gains, if there is any practical benefit in doing so. For example, the paralleling of two tubes is often used as a device to double the power; it may be just as desirable to run two Amplitrons in cascade to produce increased power although the gain of the second tube may be only 3 db.

Experimental study of high level drive of the QK520 Amplitron reveals that the advantages of extremely high efficiency and extremely high power output are to be gained through high level drive, low gain operation of these tubes. Efficiencies of Amplitrons run under these conditions were measured very carefully by the heat-balance method in which anode dissipation power as well as output power are calorimetrically measured. These results were then checked against efficiency computed by the usual method of dividing the calorimetrically measured rf power output by the modulator power output. It was concluded that measured efficiencies were not less than 71.3 nor greater than 76% for several operating conditions where the power exceeded 1600 kw. Observed data are tabulated in Table II.

F. Phase and Characteristic Impedance Properties

The phase shift vs frequency characteristic of the platinotron is necessary in the determination of the phase velocity of the space harmonic interacting with the electrons. But in the examination of the circuit for this characteristic, it will be convenient to discuss the characteristic impedance of the platinotron circuit as well. The strapped structure, common in magnetrons and in many of the platinotron structures which have been built, will be discussed, with the full realization that similar expressions can be developed for other structures.

Figure 13 shows a section of the strapped circuit. If we regard the two straps as a parallel transmission line with the platinotron cavities representing impedances hung across the transmission line as loading, we obtain an equivalent circuit as shown in Fig. 13, where L_s represents the strap inductance between cavity sections, C_s the capacity between the two straps, and Z_c the input impedance to the cavity across the points of strap connection, for example, points A–D. Z_c may be considered as nearly purely reactive. This equivalent circuit behaves as a two-terminal

TABLE II

AMPLITRON (QK520) HIGH EFFICIENCY DATA UNDER CONDITIONS OF HIGH RF DRIVE

Magnetic field (gauss)	Anode potential (kv)	Anode current (ma)	Total average power output (watts)	Amplitron average power output (watts)	Amplitron anode dissipation (watts)	Efficiency method A[a] (%)	Efficiency method B[b] (%)
1260	39.0	26	1370	760	312	75.0	71.0
1260	39.6	31	1560	950	356	77.5	72.8
1260	40.9	36	1710	1100	445	75.0	71.3
1260	42.7	41	1920	1310	535	75.5	71.3
1330	42.1	31	1600	990	338	76.0	74.5
1395	44.7	31	1640	1030	356	74.7	74.5

[a] Method A—efficiency $= \dfrac{\text{(rf power out} - \text{rf power in)}}{\text{(modulator kv)(modulator av. current)}}$

[b] Method B—efficiency $= \dfrac{\text{(rf power out} - \text{rf power in)}}{\text{(rf power out} - \text{rf power in)} + \text{anode dissipation}}$

Conditions of operation

duty cycle	0.001
pulse duration	5 μsec
rf drive power	610 kw
frequency	1300 Mc
load condition	matched

Note: Input drive power was measured at output of Amplitron with Amplitron turned off. Use of same power meter to measure both power output and power input minimized any effect of an error in the carefully calibrated calorimetric power meter upon efficiency.

pair network with band-pass characteristics. The lower cutoff of the pass band occurs at a frequency where Z_c and C_s resonate in parallel, that is, where $Z_c = -j/\omega C_s$ and the upper cutoff occurs when

$$\frac{2Z_c}{1 - j\omega C_s Z_c} = -j\omega L_s$$

From network theory the phase shift function is given as

$$\theta = \cos^{-1}\frac{Z_{11}}{Z_{12}} = \cos^{-1}\left(\frac{j\omega L_s + (Z_c/1 + j\omega C_s Z_c)}{Z_c/1 + j\omega C_s Z_c}\right) \tag{3}$$

$$\theta = \cos^{-1}\left\{\frac{j\omega L_s}{Z_c}\left[1 - \left(\frac{\omega}{\omega_c}\right)^2\right] + 1\right\} \tag{4}$$

where ω_c is defined as the lower cutoff frequency, that is, $\theta = 0$. The characteristic impedance function is given as

$$Z_0 = \sqrt{Z_{11} - Z_{12}} \tag{5}$$

$$Z_0 = \sqrt{j\omega L_s \left(j\omega L_s + \frac{2Z_c}{1 + j\omega C_s Z_c} \right)} \tag{6}$$

The phase shift and the characteristic impedance functions are shown in Fig. 14 for a particular choice of circuit parameters in which Z_c is assumed to consist of a lumped inductance and capacity. In general Z_c will not be a simple function of frequency (*3*). The phase shift across the network will be zero at the lower cutoff frequency and π radians at the upper cutoff frequency. There will usually be a substantial range in which the phase shift is nearly linear with frequency. The characteristic impedance is infinite at the lower cutoff frequency and zero at the upper cutoff frequency.

G. Conditions for Synchronism

Having obtained the phase shift θ as a function of frequency for the network, it is possible to investigate the synchronism relationship between

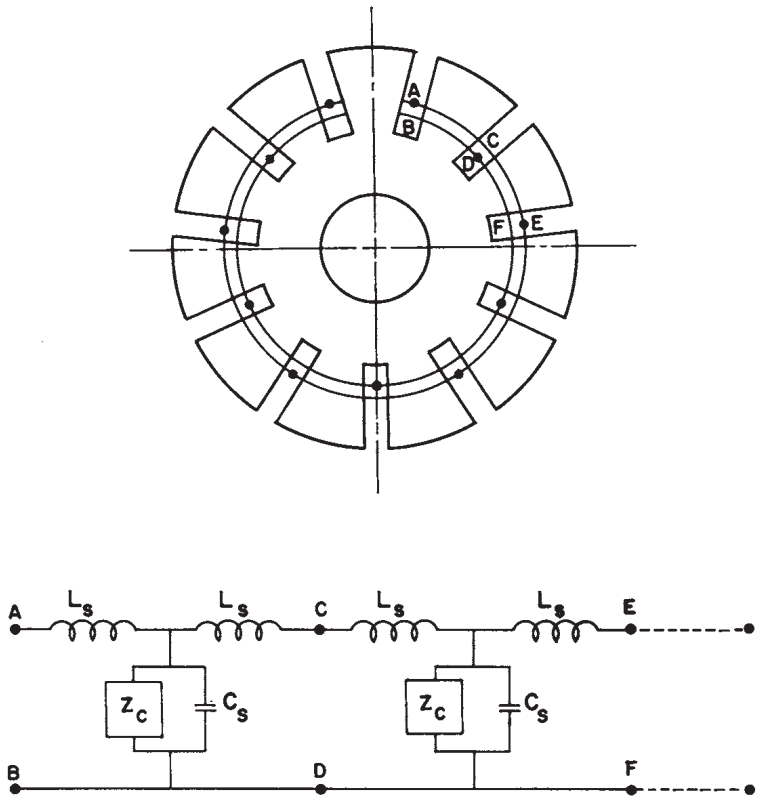

Fig. 13. The platinotron circuit and its two-terminal-pair network representation.

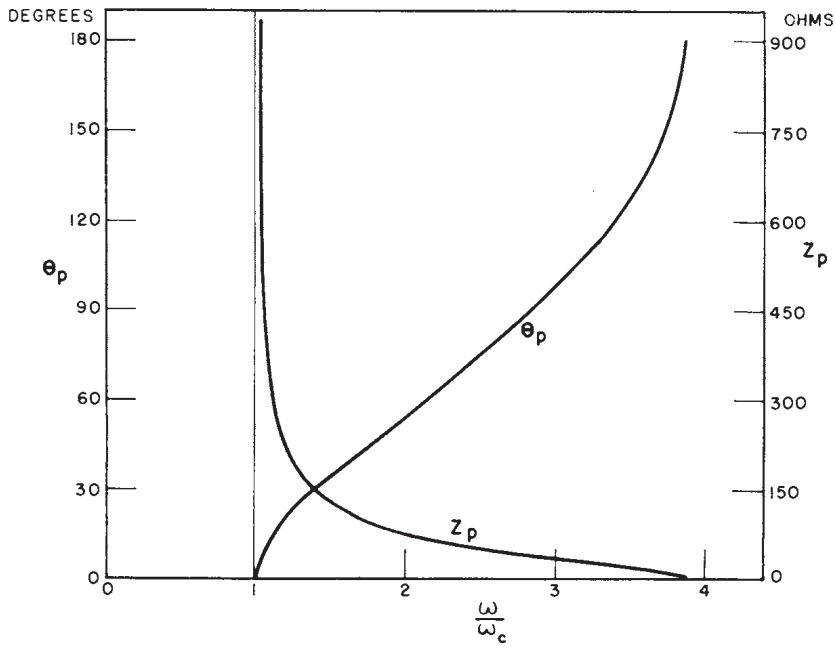

FIG. 14. Theoretical phase shift and characteristic impedance functions typical of the network representation of Fig. 13.

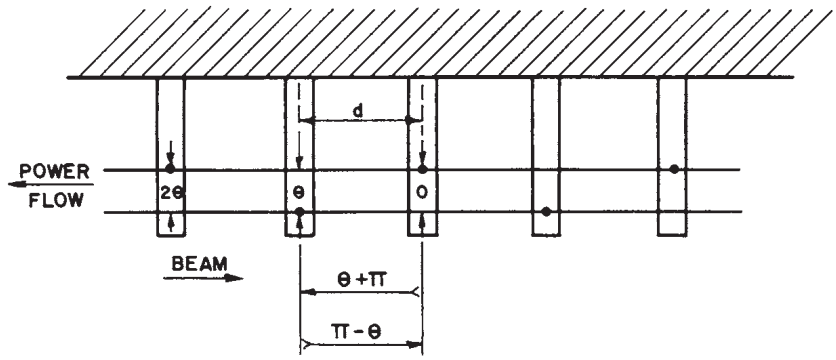

FIG. 15. Diagram illustrating conditions for interaction of the beam with a wave traveling in a direction opposite to that of the beam.

$$\lambda_s = \frac{2\pi d}{\pi - \theta} = \text{distance of one cycle of rf}$$

$$v = \frac{\lambda_s}{t} = \lambda_s f = \frac{\omega d}{\pi - \theta} = \text{phase velocity}$$

For synchronism, phase velocity = electron velocity

$$V_0 = \frac{1}{2}\frac{m}{e}v^2 = \frac{1}{2}\frac{m}{e}\left(\frac{\omega d}{\pi - \theta}\right)^2$$

the electron beam and the traveling wave on the circuit. Figure 15 indicates a section of the network in which the direction of power flow in the circuit is indicated as being toward the left and the direction of the beam toward the right. The reversed directions of electron motion and power flow in the circuit are necessary conditions for backward wave interaction. The phase shift per network section, as given by (4) is in the direction of power flow. This phase shift is along the straps. To convert this to a phase shift in the interaction area it is necessary to add or subtract π radians because of the manner in which the vanes are connected to the straps. Since θ is always less than π, the subtraction of π radians from θ will mean a phase shift in the interaction area in the direction of the beam.

If d is the distance between vane tips, then

$$\lambda_s = \frac{2\pi d}{\pi - \theta} = \text{distance of 1 rf cycle} \tag{7}$$

$$v = \frac{\omega d}{\pi - \theta} = \text{phase velocity} \tag{8}$$

Then for synchronism the electron velocity must match the phase velocity and we have

$$V_0 = \frac{1}{2}\frac{m}{e}\left(\frac{\omega d}{\pi - \theta}\right)^2 \tag{9}$$

which gives the voltage through which the electrons must be accelerated to reach the required velocity.

H. Design Considerations

It has been determined that the QK434 platinotron in the power range where performance characteristics have been described, operates in a backward wave mode, that is, there is interaction between a backward wave space harmonic of the circuit and the rotating electron beam.

To examine this interaction quantitatively it is necessary to examine the relationship between the circuit properties of the network, the electric potential and magnetic field applied to the platinotron, and the dimensions of the interaction area between cathode and anode. The assumption that there is synchronism between the rotating space charge and the phase velocity is basic to this relationship.

In order to interrelate the magnetic field, dc potential applied to the anode, and platinotron physical dimensions, the assumption is made that there will be no interaction until synchronism between the traveling wave on the circuit and the fastest moving electrons is reached, and that further interaction will be maintained at such synchronism. How-

ever, it is not at all necessary for the electrons to be located at the tips of the vane for effective interaction and, for efficiency considerations, it is quite necessary that the synchronism condition be established early in the movement of the electron from the cathode to the anode. Equations (10)–(12) relate the voltage at which operation begins to the physical dimensions of the tube and value of magnetic field. These equations will be recognized as being similar to the design equations for magnetrons with the difference that $N(\pi - \theta)/2\pi$ has been substituted for the mode number n.

$$V = V_0 \left(2 \frac{B}{B_0} - 1\right) \text{ volts} \tag{10}$$

$$V_0 = 253{,}000 \left[\frac{2\pi r_a}{N(\pi - \theta)/2\pi}\right]^2 \text{ volts} \tag{11}$$

$$B_0 = \frac{21{,}200}{N\left(\frac{\pi - \theta}{2\pi}\right)\lambda\left[1 - \left(\frac{r_c}{r_a}\right)^2\right]} \text{ gauss} \tag{12}$$

where

V = threshold voltage or where operation starts,
V_0 = value of voltage between anode and cathode, which, with a field of B_0, causes the electrons to just graze the anode at synchronous velocity,
B_0 = value of magnetic flux for grazing of anode by electrons at synchronous velocity,
B = value of magnetic flux in Gauss,
r_a = radius of anode in centimeters,
λ = operating wavelength of tube in centimeters,
N = number of vanes (assumed equally spaced),
θ = phase shift along straps of the network as defined in (4).

I. Bandwidth Considerations

The platinotron may not operate equally well at all values of θ because of the electron re-entrancy involved. Consider, for example, attempting to operate an odd numbered vane platinotron in the π-mode. Figure 16 should make it clear that in the π-mode ($\theta = 0$) electrons which are bunched to deliver energy to the traveling wave at the input of the network will take energy from the traveling wave at the output of the network after traversing the gap between input and output. Such a situation may not be conducive to a satisfactory interaction between electrons and a circuit traveling wave, although it is conceivable that the unfavorably bunched electrons could regroup themselves and move into a region of favorable phase.

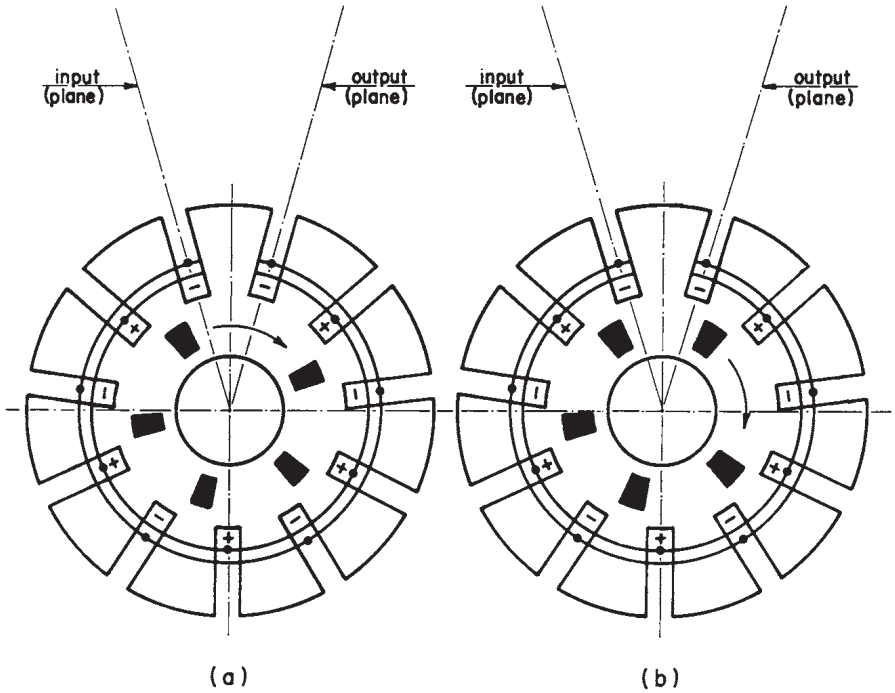

FIG. 16. Diagram illustrating poor conditions for interaction of the spokes of space charge with the platinotron circuit. (a) Electrons all bunched to deliver energy to the traveling wave. (b) One cycle of rf later when first group of electrons is accepting energy from the traveling wave.

On the other hand, if there is an approximately 180 deg phase shift along the straps from output to input, the bunched electrons will deliver energy to the circuit on either side of the gap between output and input. This situation is favorable to the proper operation of the platinotron.

The general requirements for the electron bunches to be in phase with the traveling wave on both sides of the gap can be derived. Consider a bunch of electrons located at the output plane shown in Fig. 16 at time $t = 0$. Then if t' is the time required for this group of electrons to rotate around the cathode once and come back to the output plane, the phase change at the output plane is obviously $\omega t'$. And, of course, if the electrons and the traveling wave are to have the same phase relationship at t' as at $t = 0$, $\omega t'$ must be an integral multiple of 2π.

$$\omega t' = M2\pi \tag{13}$$

where M is an integer.

Now t' is equal to the distance around the anode divided by the velocity of the electron bunches. This velocity is the phase velocity v given by (8). Then

$$t' = \frac{2\pi r_a}{v} = \frac{2\pi r_a}{\omega d/\pi - \theta} = \frac{N(\pi - \theta)}{\omega} \text{ sec} \tag{14}$$

Substituting the expression for t' into (13) we obtain

$$\theta = \pi\left(1 - \frac{2M}{N}\right) \text{ radians} \tag{15}$$

If the electrons after crossing the gap are permitted to initially lead or lag the traveling wave on the circuit, additional equations may be derived to determine the corresponding phase shifts permitted on the network.

$$\theta_{max} = \pi\left[1 - \frac{2(M - Q)}{N}\right] \tag{16}$$

$$\theta_{min} = \pi\left[1 - \frac{2(M + Q)}{N}\right] \tag{17}$$

where

$$Q = \frac{\text{lead or lag of beam (deg)}}{360}$$

J. Application of Design Considerations

The QK434 is the experimental platinotron developed under Signal Corps contract. It was designed for use at L-band and for a peak output power level of 200 to 1000 kw. A considerable amount of data have been taken with this tube being used as both an Amplitron and a Stabilotron. It is, therefore, logical to use this tube to illustrate various aspects of platinotron design and performance.

A plan and cross section view of the interaction area of the QK434 platinotron is shown in Fig. 3. Pertinent dimensions are as follows:

Number of vanes = 11
Cathode diameter = 0.750 in.
Anode diameter = 1.600 in.
Vane length = 1.500 in.

The experimental phase shift vs frequency curve for the entire network of ten cavities of the configuration shown in Fig. 4 has been found to be as shown in Fig. 17. The formula given by (4) for a single network section is difficult to apply for vanes of this geometry because of the difficulty of determining Z_c as a function of frequency. If, however, Z_c is assumed to be the impedance of a lumped circuit element, which must be inductive in nature, it is possible to compute the value of L_c using the experimental lower cutoff frequency and one other point from the 1200–1400 Mc region of the phase shift vs frequency characteristic. If the values of ωL_c so obtained are then used for Z_c in (4), the agree-

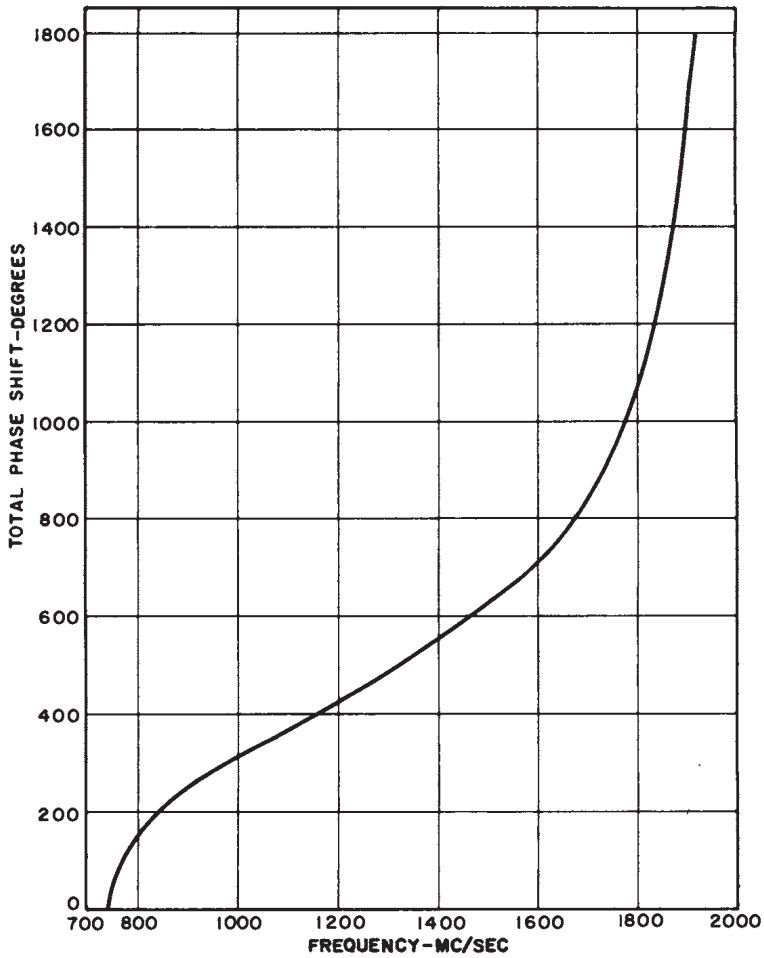

FIG. 17. Experimentally determined phase shift across the platinotron (QK434) network of ten sections as a function of frequency.

ment between the experimental curve and that predicted by (4) will be excellent in the frequency region up to 1500 Mc. Beyond this frequency, however, there is serious lack of agreement.

With the aid of the phase shift vs frequency characteristic given in Fig. 17, it is possible to apply (15)–(17) to determine the preferred frequencies of operation. The results are shown in Fig. 18. Equation (14) may be solved for the values of the phase shift across each network section which will permit the re-entrant electron beam to re-enter the input side of the circuit in exact synchronism with the circuit wave. These values of phase shift are found to be 17° and 49° and higher values not shown in Fig. 18. The platinotron will operate satisfactorily at either of the two frequencies determined by the two respective phase

shifts. Figure 18 also shows in heavy shading the frequency regions determined by (16) and (17) for a 45° lag and lead of the re-entrant beam, and in lighter shading the frequency regions determined by a 90° lag and lead of the re-entrant beam.

It is not clear from an examination of Fig. 18 whether operation at 800 or 1300 Mc is to be preferred. Because the 1300 Mc region represents a frequency region of interest to radar systems, most of the experimental data have been taken in this frequency region of operation, although very efficient operation has been observed in the 800 Mc region.

From the dimensions given for Fig. 4, from the phase shift and frequency as determined by (4) and Fig. 17, and from Eqs. (10)–(12), it is possible to determine the relationship between anode potential and magnetic field for the onset of operation for backward wave interaction. The relationship between this threshold voltage and the magnetic field for a frequency of 1300 Mc is given as the upper curve in Fig. 19. The lower curve in Fig. 19 indicates the predicted relationship between anode

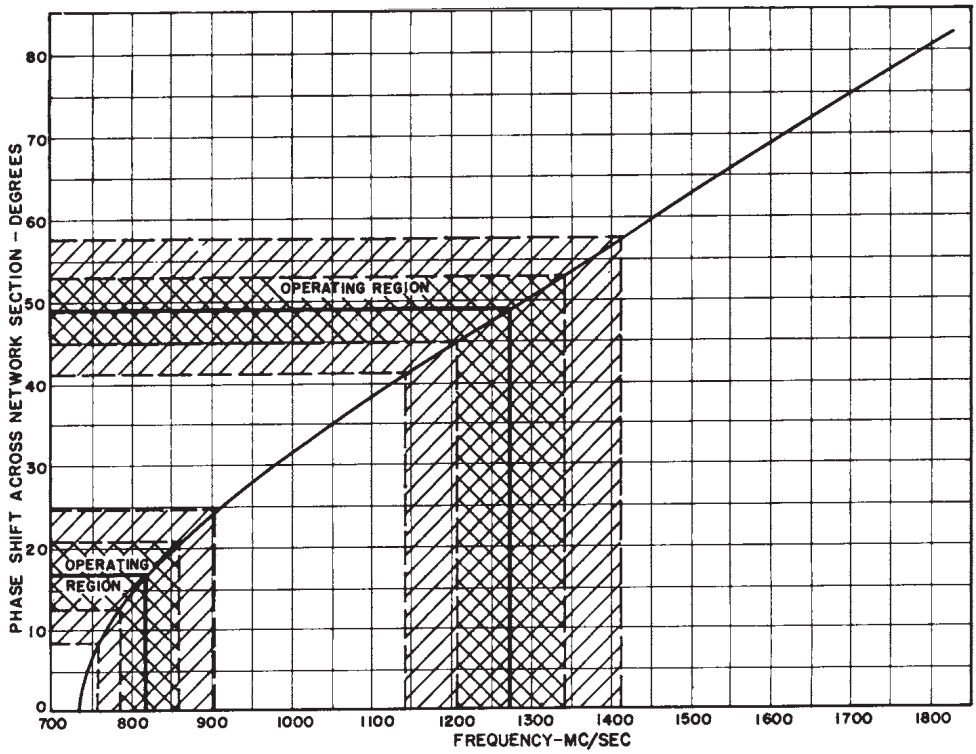

FIG. 18. Diagram illustrating regions of phase shift and frequency in which operation of the platinotron (QK434) may be expected. Heavily cross-hatched regions correspond to a 45° lead or lag of the rotating spokes. Lightly cross-hatched regions correspond to a 90° lead or lag.

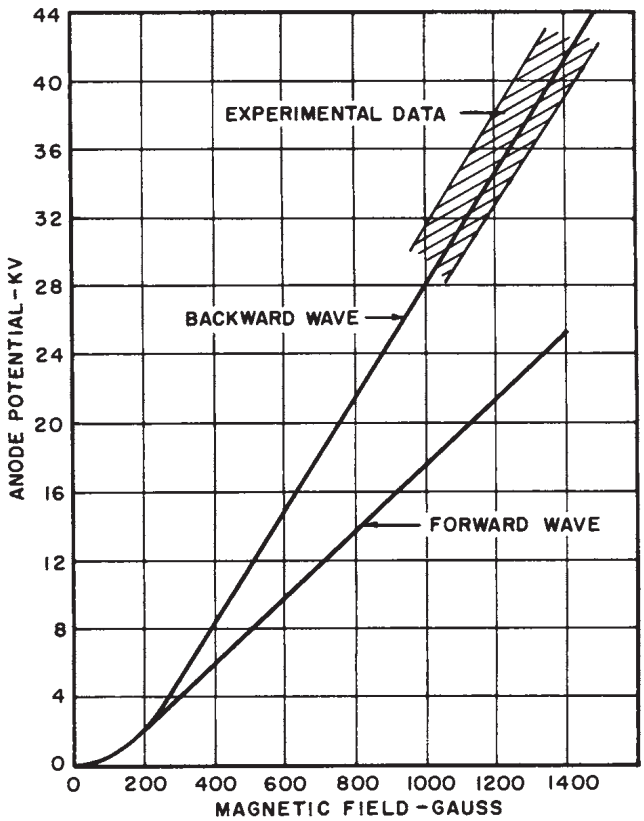

FIG. 19. Theoretically predicted and observed relationship between anode potential and magnetic field for onset of platinotron (QK434) operation. Cross-hatched area contains points of experimentally observed behavior.

potential and magnetic field for interaction with the forward wave at 1300 Mc. Equations (10)–(12) can be converted to predict forward wave interaction by adding θ to π in the equations instead of subtracting it.

In the region of rf input levels over 2.5 kw, the experimentally observed values of threshold voltage appear in substantial agreement with the predicted values for backward wave interaction. The range covered by these experimental data is also indicated on Fig. 19. However, at lower rf input levels forward wave interaction has been observed at current levels from 0 to 3 amp.

The proper operation of the platinotron is dependent upon a reasonable impedance match between the platinotron network and the input and output terminals over a reasonable range of frequency. For suitable tube geometries (6) may be used to compute the characteristic impedance. For the QK520 the characteristic impedance at 1300 Mc was experimentally found to be 92 ohms. Although considerable work has

been expended on the matching problem, such problems are common to a variety of microwave tubes, and so need not be discussed in detail here. The broad-band match, which was obtained for the QK520, is shown in Fig. 20. The VSWR as given in Fig. 20 is that VSWR obtained by looking into the input to the platinotron with the output pipe looking into a matched-load.

III. The Stabilotron

A. Performance Characteristics

The Stabilotron is a relatively new device and performance data are therefore limited. Most of the data available are for a 500 kw tube in the L-band region. However, the Stabilotron obeys the scaling laws, so that extrapolation to other frequencies and power levels can be accomplished. For a given frequency and power level, Stabilotrons have the same size cathodes and anodes as magnetrons, and over-all sizes and magnet requirements are comparable.

Figure 21 is illustrative of the type of performance which may be obtained from a Stabilotron over a wide frequency range. Efficiency, which is defined as useful rf output to modulator output, remains substantially flat and over 45% across the 1250–1360 Mc tuning range. Across the frequency band the pulling was less than 0.5 Mc and the pushing figure less than 10 kc/amp in the region of operation.

A representative Rieke or load diagram is shown in Fig. 22 and a performance chart is shown in Fig. 23. The same stabilizing cavity was used to obtain the data for Figs. 21–23.

The very great increase in frequency stability of the Stabilotron over a conventional magnetron is demonstrated in Figs. 24a–24c. Figure 24a shows a poor current pulse, 17 μsec wide, with an unusual amount of

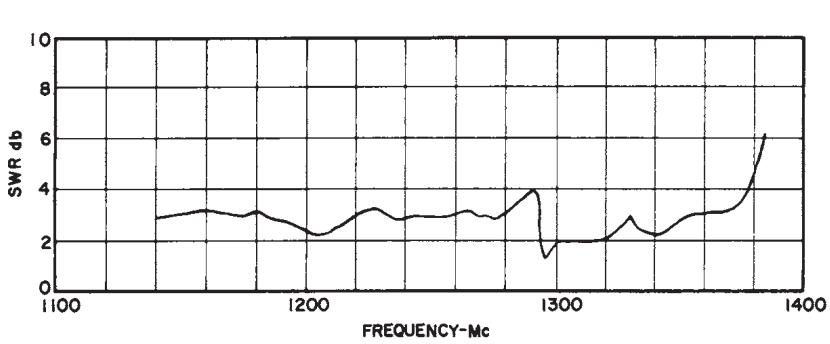

Fig. 20. Broadband match between the external circuit and the platinotron (QK434).

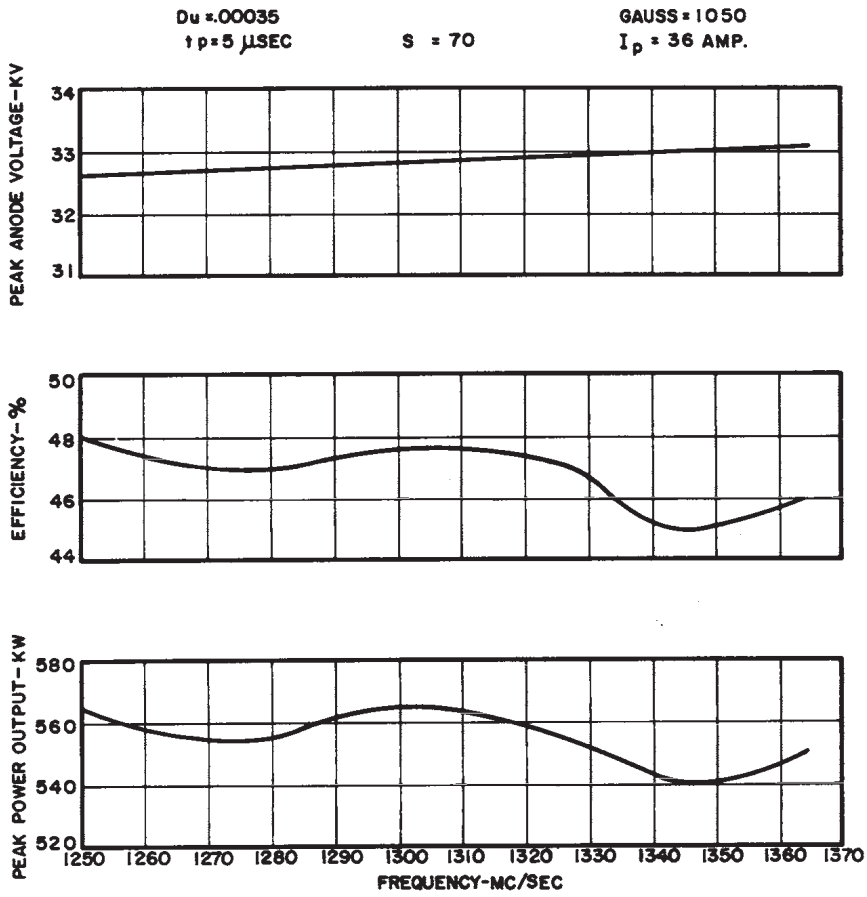

FIG. 21. Stabilotron (QK434) anode voltage, efficiency, and power output vs frequency characteristics. Load matched. Constant magnetic field and anode current. Stabilization factor of 70.

current variation, which was the response of both a 5J26 magnetron and the QK434 Stabilotron to the modulator voltage pulse. Figure 24b shows the output spectrum of 5J26, more than ten times the theoretical width for a 17 μsec pulse. Figure 24c shows the output spectrum of the QK434 Stabilotron which was very near theoretical. Note that the frequency scales are different for the two figures so that the improvement is about three times greater than would be indicated by visual comparison of the pictures. This improvement was largely brought about by a 50-to-1 improvement in the ratio of frequency change to current change.

Stabilotrons have a number of advantages resulting from this greatly increased frequency stability. One direct result is that the same high tube efficiencies can be obtained at X-band and K-band as at S-band.

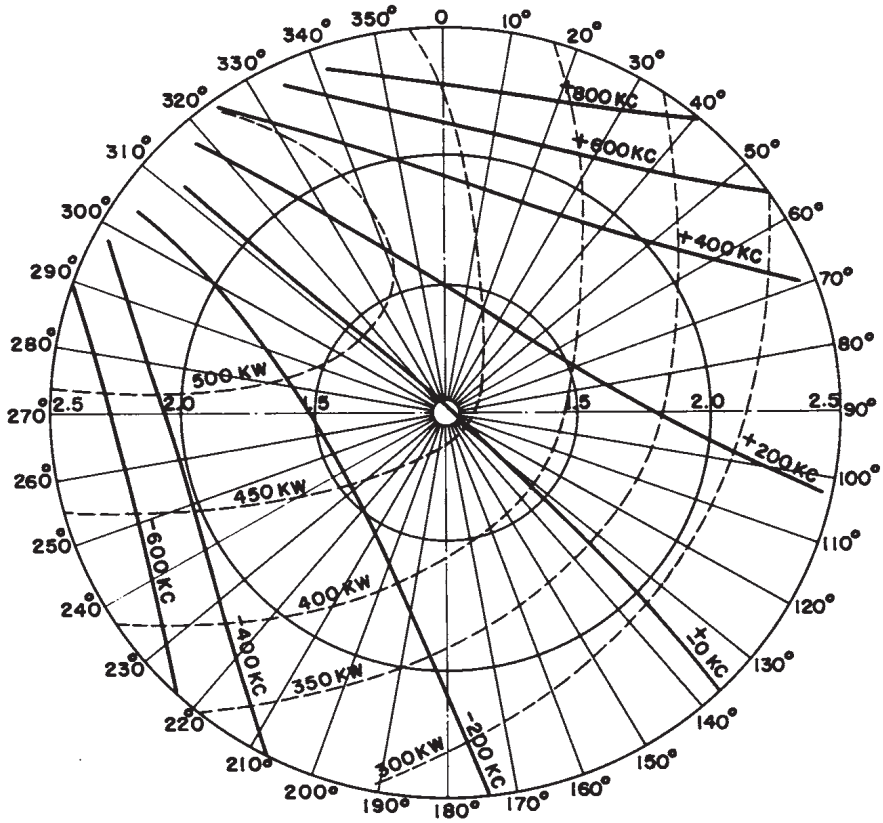

FIG. 22. Stabilotron (QK434) load diagram at 1300 Mc/s. Stabilization factor of 70. Internal mismatch 4/1, line stretcher on input. Magnetic field 1050 gauss, pulse width 5 μsec, applied voltage 32 kv, anode current 30 amp, duty 0.00035.

At the present time it is customary to design for lower efficiencies at these high frequencies in order to preserve some frequency stability in terms of pushing and pulling figures.

Another result of the increased frequency stability is that long pulse lengths of the order of 20 to 40 μsec appear to be practical in the L-band region or below.

B. CIRCUIT ANALYSIS

The Stabilotron consists essentially of four different elements as illustrated in Fig. 25, namely: the platinotron amplifier tube, a stabilizing cavity system, an output reflection, and transmission lines joining the parts together. The impedance of the transmission lines are matched to the characteristic impedance of the broadband network of the platinotron amplifier over a wide range of frequencies.

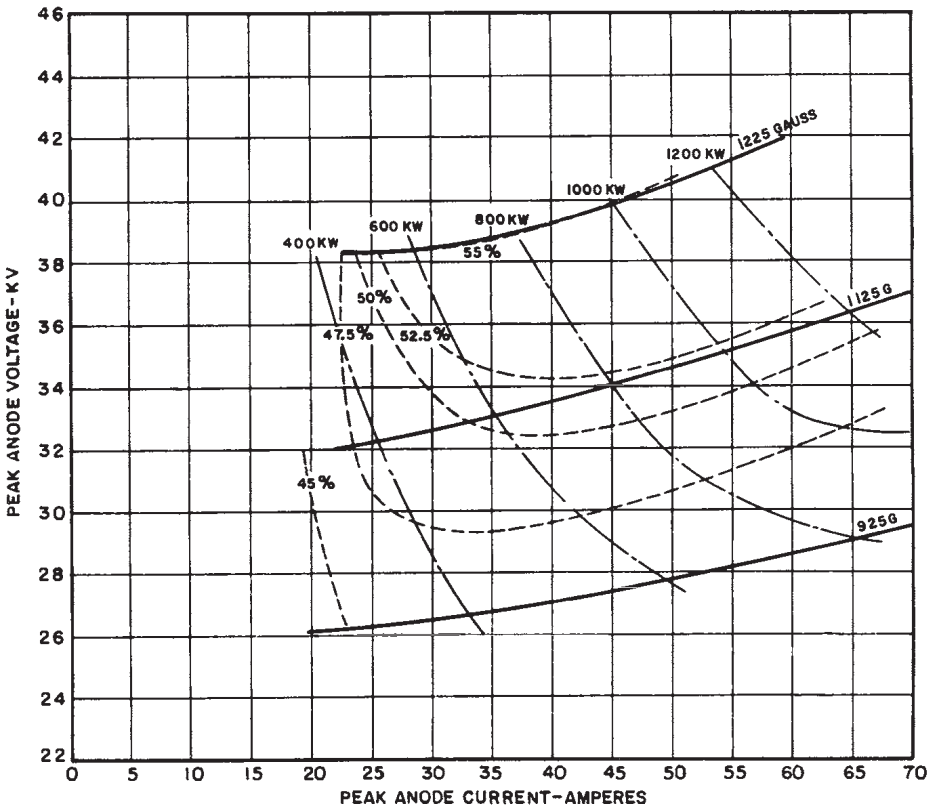

FIG. 23. Stabilotron (QK434) performance at 1300 Mc/s. Stabilization factor of 70. Pulse width 3 μsec and duty 0.001.

Figure 26 provides a basis for describing the manner in which the Stabilotron circuit operates. A portion of the output power is reflected from the reference plane ll'. This reflected power travels back through the anode with little or no attenuation or reflection and out to reference plane rr' where most of it is again reflected, the phase of the reflection depending upon the frequency of the wave and the resonant frequency of the stabilizing cavity. This re-reflected power is then amplified by the backward wave principle and arrives at the reference plane ll', at full output level. It will be realized that steady oscillations can occur only if the loop phase shift from plane ll' to plane rr' and return is an integral multiple of 360°. The phase shift vs frequency characteristic of the stabilizing cavity has a slope many times greater than that of any other element in the circuit. Hence a slight change in frequency will permit the cavity to correct for a substantial phase shift which might be introduced by a change in the antenna load, by frequency pushing of the electron stream, etc.

It will be noted in Fig. 26 that there are four different factors which

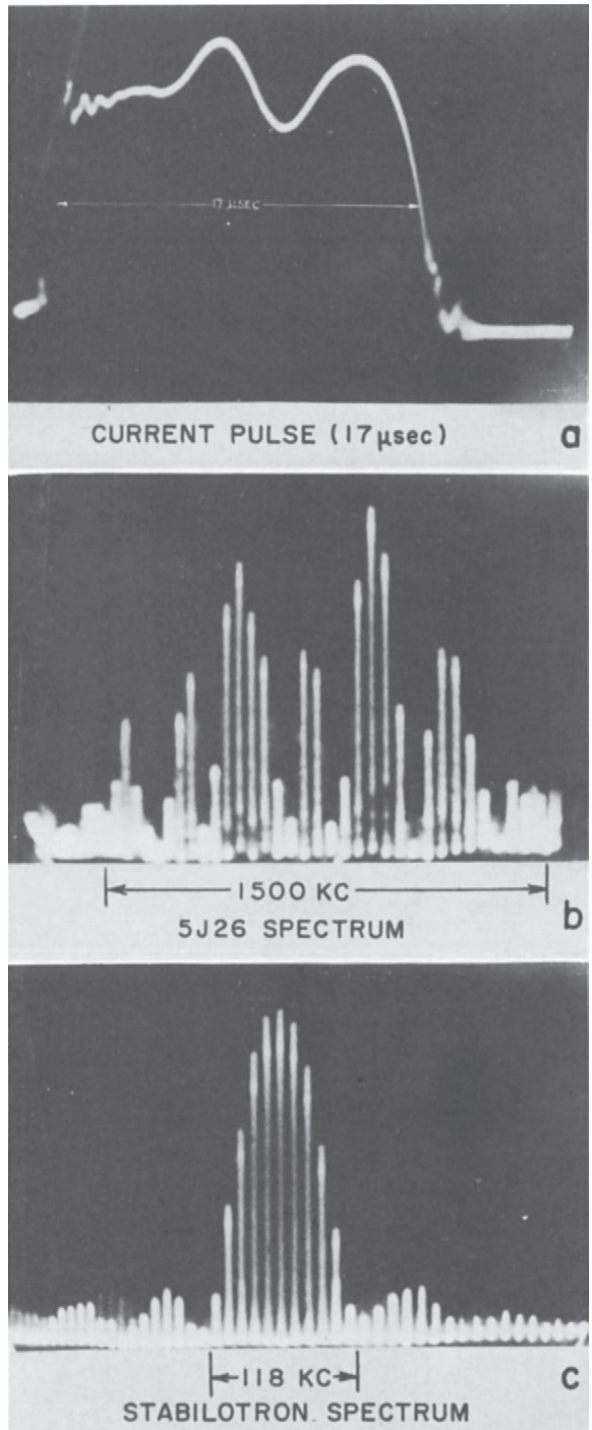

FIG. 24 (a). Applied pulse-current vs time-characteristic. (b). Conventional magnetron spectrum. (c). Typical Stabilotron spectrum.

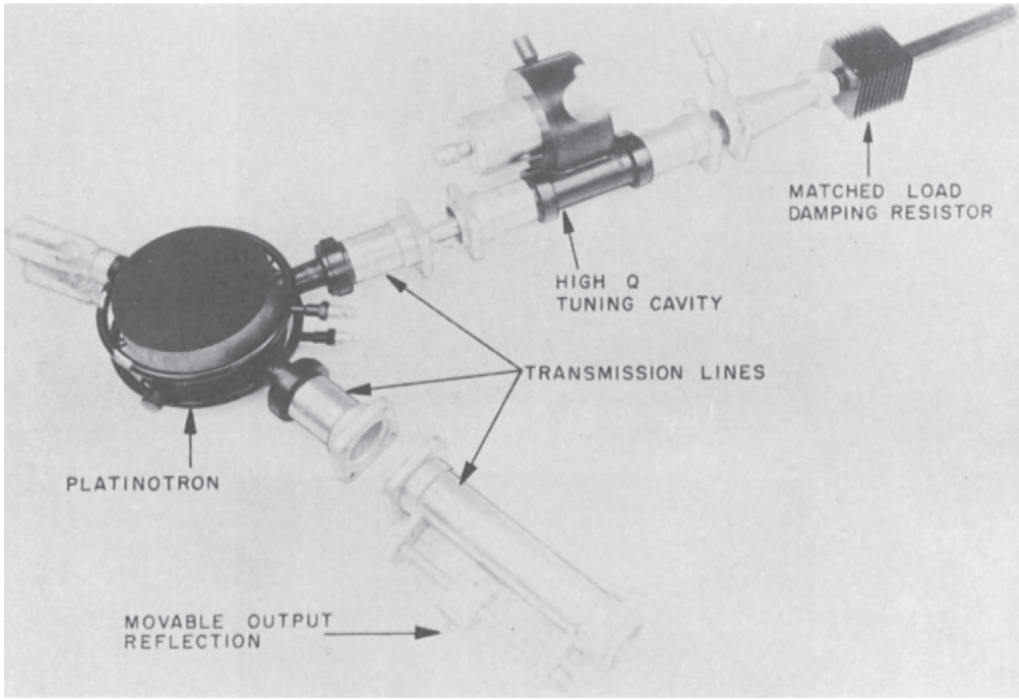

FIG. 25. Stabilotron components.

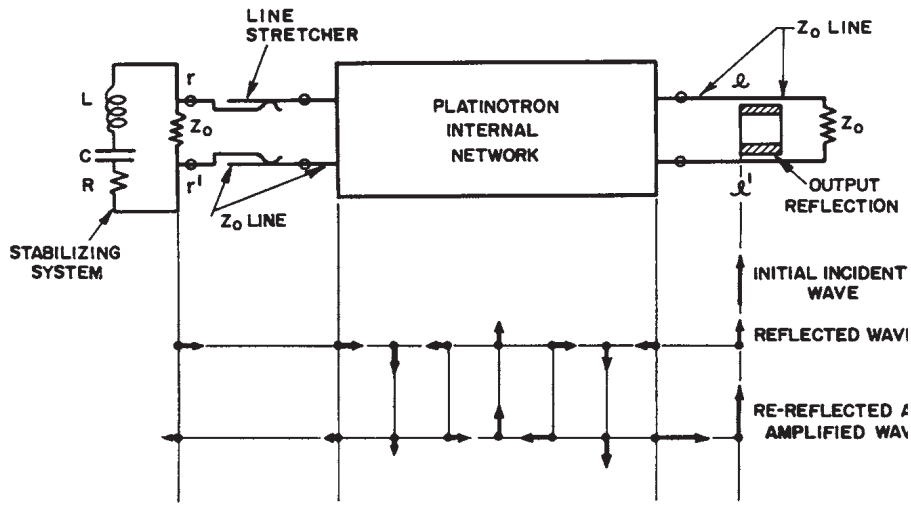

FIG. 26. Stabilotron basic schematic diagram.

contribute to the total loop phase shift. These factors are: the phase shift within the backward wave amplifier tube or platinotron itself, the phase shift which takes place at the reference ll', the phase shift which takes place at the reference plane rr', and the phase shift which occurs in the transmission lines which connect the platinotron or backward wave amplifier with the reference planes rr' and ll'. The phase shift occurring in each of these elements is a function of frequency.

Figure 27 shows how these individual phase shifts add up to give a total loop phase shift which is again a function of frequency. The system will oscillate at a frequency where the total loop phase shift θ_α is an integral multiple of 2π radians. It is clearly indicated in Fig. 27 that the phase shift vs frequency characteristic of the stabilizing cavity in the region of cavity resonance has a slope many times greater than any

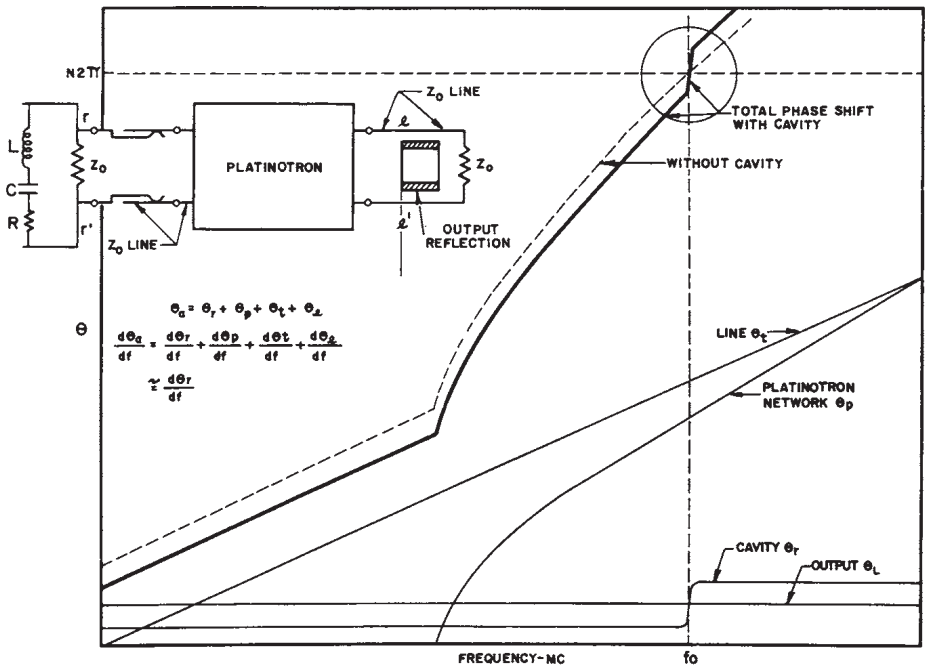

FIG. 27. Phase shift vs frequency characteristic. The diagram illustrates how the various components contribute to the total phase shift characteristic whose interaction with an $N2\pi$ phase value determines frequency of operation.

other element in the circuit. The tube oscillates in this region of steep slope because of the damping resistor, shown as the resistor Z_0 in Fig. 26, which effectively absorbs all incident energy unless it be at a frequency close to that of the resonant frequency of the cavity, leaving no reflected signal for excitation of the amplifier. As will be demonstrated in the next paragraph, it is the steep slope of the phase shift vs frequency characteristic of the cavity which gives the over-all system its high degree of frequency stability.

The phase shift vs frequency characteristic in the region of this steep slope is examined with the aid of Fig. 28, which is an expansion of the encircled area of Fig. 27. In general any instability which tends to change the frequency of the system can be represented by a small incremental phase shift $\Delta\theta$ which will either raise or lower the total phase shift θ_α and thus cause it to intersect the required loop phase shift $N2\pi$

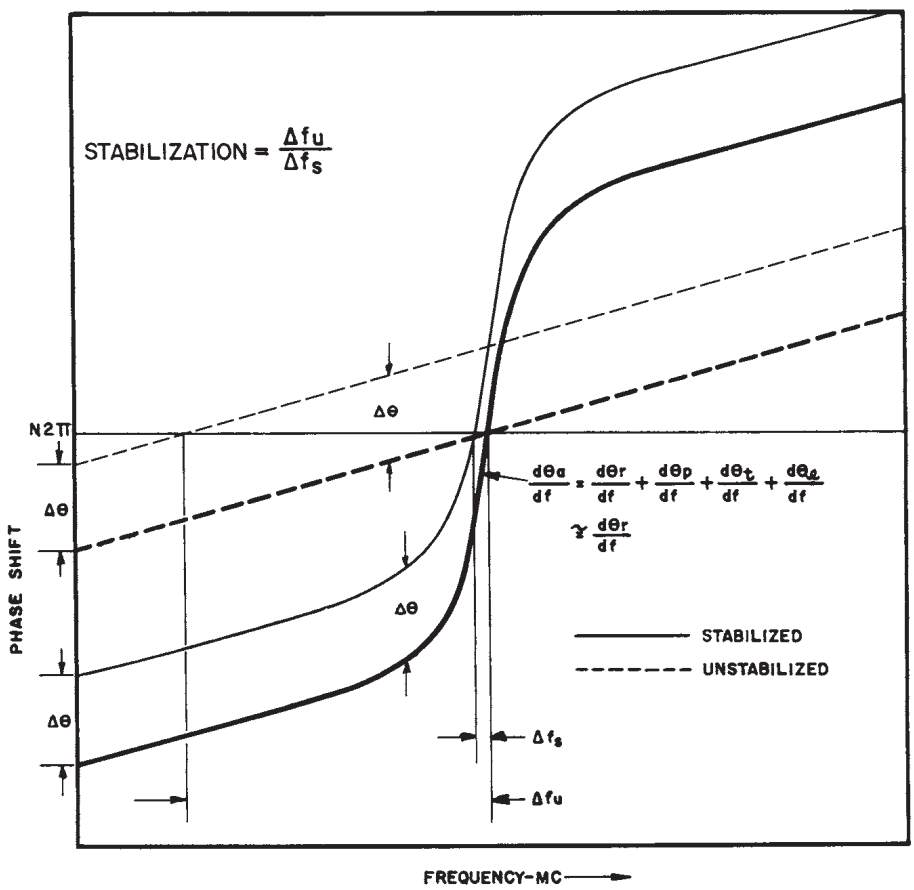

FIG. 28. Phase shift vs frequency characteristic (expanded from Fig. 27). Stabilizing action of cavity is illustrated.

at a different frequency. Figure 28 demonstrates the frequency shift which occurs for the same $\Delta\theta$ phase shift in a stabilized and unstabilized system. It is clearly evident in Fig. 28 that a very steep slope of θ_α in the region of $N2\pi$ phase shift reduces the corresponding frequency shift. It would be possible to say from examination of Fig. 28 that the frequency stabilization that has been introduced is equal to $\Delta f_u/\Delta f_s$ where Δf_s and Δf_u are the frequency shifts taking place in the stabilized and unstabilized systems, respectively, for the same incremental disturbance $\Delta\theta$ in the total phase shift.

Having determined that it is the disturbance in the total phase shift which causes the frequency instability in the system, it is necessary to demonstrate the relationship between $\Delta\theta$ and various factors which cause such instability in the system. In general, these factors which cause instability can be divided into two classes. The first class includes the disturbances which take place in the circuit external to the Stabilotron circuit; that is, disturbances which take place to the right of the reference plane ll' in Fig. 26. A measure of the amount of disturbance from such external factors is the pulling figure, a figure of merit which has been used for many years on magnetrons. It is the maximum frequency shift in the total system which is produced by varying through all possible phases a disturbance which introduces a VSWR of 1.5 in the transmission line connecting the oscillating system to a matched load.

The second class of factors which cause instability are those factors which cause disturbance within the Stabilotron system itself; that is, those disturbances arising somewhere in the system between ll' and rr'. These consist of many different items which can in turn be classified into two broad subclasses.

The first subclass consists of instabilities caused by changes in the magnitude of the physical parameters of the platinotron circuit or transmission lines, excluding effects of the driving space charge. Examples of such changes in physical circuit parameters are expansion or contraction due to temperature changes; microphonics; deposition of cathode coating on vane tips; release of stresses, and corresponding displacements, with time and temperature; electronic tuning, if such tuning is not associated with the driving space charge; gas in cavities; and barometric effects.

The second subclass consists of those changes associated with the interaction between the driving space charge and the platinotron circuit. Such disturbing influences include frequency pushing, electron tuning, etc.

It is possible to analyze both of these two general classes of frequency disturbing influences; that is, loading effects external to the Stabilotron circuit, and disturbances occurring within the Stabilotron circuit itself. In general, it will be found that improvements in frequency stability of

different orders of magnitude will be found in the two different classes of disturbances. In the category of external disturbances, it will be found that improvements over conventional magnetron oscillators by a factor of about 10 are reasonable, whereas improvements in stability from internal disturbances by a factor of over 100 are entirely reasonable. The reasons for this will be pointed out in the analysis of the two different classes of instability.

The frequency disturbing effect of a change in external load will be examined first. Referring to Fig. 29, it will be noted that if a 1.5 VSWR is added to the external circuit, the phase θ_l of the reflection from ll' will be increased and decreased by a certain amount adding up to a total phase shift of $\Delta\theta$, and that the total phase shift θ_α will be changed by the same amount $\Delta\theta$. As can be clearly seen in Fig. 29 this change in phase produces a change in frequency of Δf. This Δf is also the pulling figure for the system since Δf has been determined by the standard test procedure for determining the pulling figure; that is, by moving a 1.5 VSWR through all possible phase positions and by noting the maximum frequency change.

The analysis of stabilization against those disturbing elements internal to the Stabilotron system is carried out with the aid of Fig. 30. Since the ultimate objective is to compare the frequency stability of the

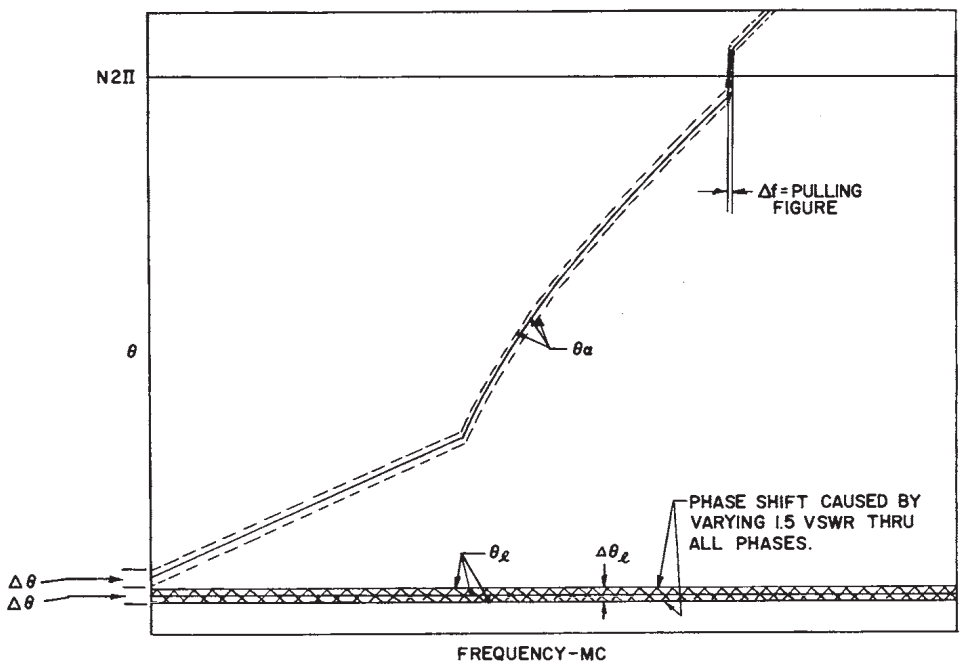

FIG. 29. Effect of external load on frequency characteristic. The pulling figure.

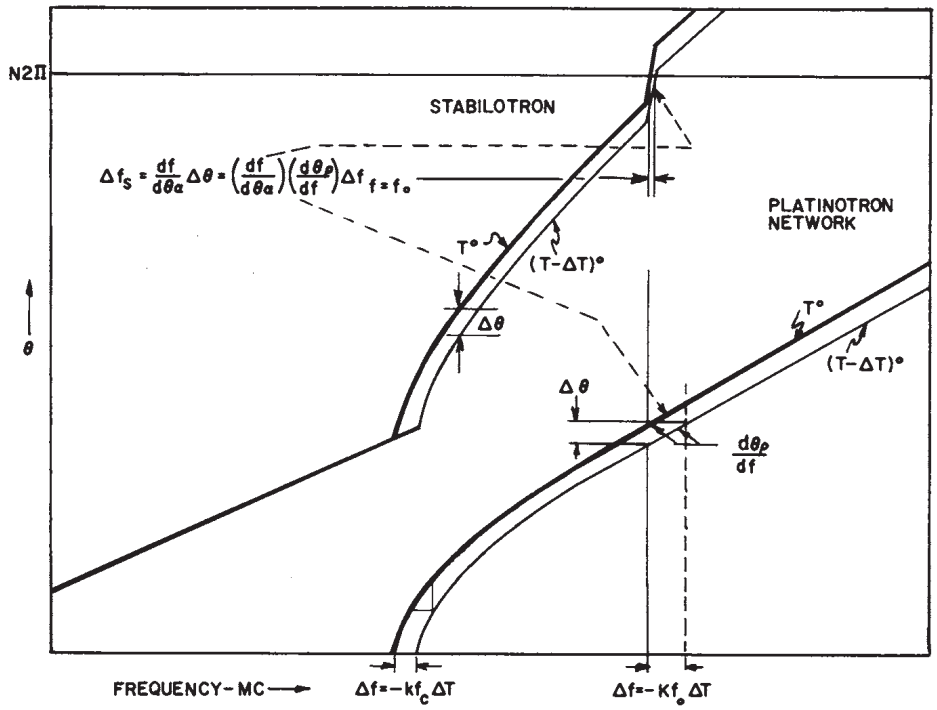

FIG. 30. Effect of stabilization on internal disturbing factors such as temperature changes.

Stabilotron system with that of the conventional unstabilized magnetron oscillator, it is desirable to carry out the analysis with this in mind. To make it more understandable to the reader, the analysis will be carried out for the frequency change which accompanies a temperature change in the platinotron circuit, but it should be remembered that the improvement in frequency stability associated with temperature change will be identical with the improvement in other forms of frequency stability associated with dimensional changes of the anode.

It is well established that the wavelength of an oscillating magnetron is proportional to its dimensions, and that if a given temperature change causes a 0.1% change in dimensions, the wavelength will also vary by 0.1%. From the small changes in dimensions associated with temperature change, it can be shown that:

$$\Delta f_{\mu\pi} = -Kf_\pi \Delta t$$

where

$\Delta f_{\mu\pi}$ = frequency shift in an unstabilized π mode magnetron
K = coefficient of thermal expansion
f_π = operating frequency, π mode
Δt = change in temperature

The effect of the Δt temperature change on the Stabilotron system, however, is entirely different. It will be noted from Fig. 30 that the phase shift vs frequency curve for the platinotron network is shifted in frequency by an amount $-Kf\Delta t$ and that this displacement at the operating frequency f_0 corresponds to $-Kf_0\Delta t$. Now the phase shift associated with this displacement in frequency is $\Delta\theta$, which is equal to $(d\theta_p/df)\ (\Delta f)$. The total phase shift θ_α is then lowered by an amount $\Delta\theta$ and the corresponding change in frequency of operation is found to be Δf_s. Hence we find that the frequency shift in the Stabilotron system is:

$$\Delta f_s = \frac{-df}{d\theta_\alpha} \cdot \Delta\theta = -\left(\frac{df}{d\theta_\alpha}\right)\left(\frac{d\theta_p}{df}\right) K\Delta t f_0$$

The corresponding frequency shift in a conventional, unstabilized π-mode magnetron has already been found to be $-K\Delta t f_0$, so that the improvement factor of the Stabilotron system over an unstabilized π-mode magnetron is found to be

$$S_{s/\mu\pi} = \left(\frac{df}{d\theta_p}\right)\left(\frac{d\theta_\alpha}{df}\right) \tag{18}$$

It will be noted from Eq. (18) that the improvement factor of the Stabilotron circuit over a conventional unstabilized π-mode magnetron depends not only upon the properties of the cavity stabilizing system (whose slope accounts for the major portion of the term $d\theta_\alpha/df$), but also upon the flatness of the slope $d\theta_p/df$, and that these two factors when multiplied together can easily give improvement factors, $S_s/\mu\pi$, of over 100. In specific instances, stabilizing factors as high as 400 might be obtained.

Although the above analysis has been carried out for the specific instance of temperature change, it is evident that it would also apply to any other factor which tended to change the physical parameters of the system, such as microphonics, deposition of cathode coating on vane tips, etc.

The reduction in pushing figure, $\Delta f/\Delta I$, which could be expected in the Stabilotron has not been discussed. Pushing in the magnetron and in the platinotron is very difficult to analyze quantitatively, so that at present comparisons are limited to experimental data. It appears, however, that the pushing figures in an unstabilized Stabilotron and in an unstabilized π-mode magnetron tend to be comparable; therefore, the improvement factors in pushing that can be obtained in a Stabilotron depend upon the product of the value $S_{s/\mu\pi}$ used and an adjustment factor ranging in value from 0.2 to 2, giving improvement factors ranging from 20 to over 100.

C. A Frequency-Tunable Stabilized System

The Stabilotron is capable of being simultaneously tuned and stabilized by one cavity. If the stabilizing cavity of Fig. 26 is tuned to a lower frequency, we have the situation as shown in Fig. 31 where the new operating frequency is $f_{0'}$. If the encircled area of Fig. 31 is expanded to obtain a more detailed picture of what is happening as the cavity is tuned, as shown in Fig. 32, it is immediately evident that some of the stabilizing influence of the cavity has been lost as denoted by the decreased slope at the operating frequency. This loss does not become serious until a considerable amount of tuning has been obtained.

In addition to the small loss in stabilization when the operating frequency of the system is removed from the resonant frequency of the cavity, a great deal more of the incident power will be absorbed in the stabilizing system. This increased absorption of power by the stabilizing system has several implications. First, the over-all efficiency of the Stabilotron will be reduced; secondly, power dissipation problems in the damping resistor portion of the stabilizing system will be increased; and finally, because of reduced reflection of the incident power, the gain requirements on the platinotron will be increased.

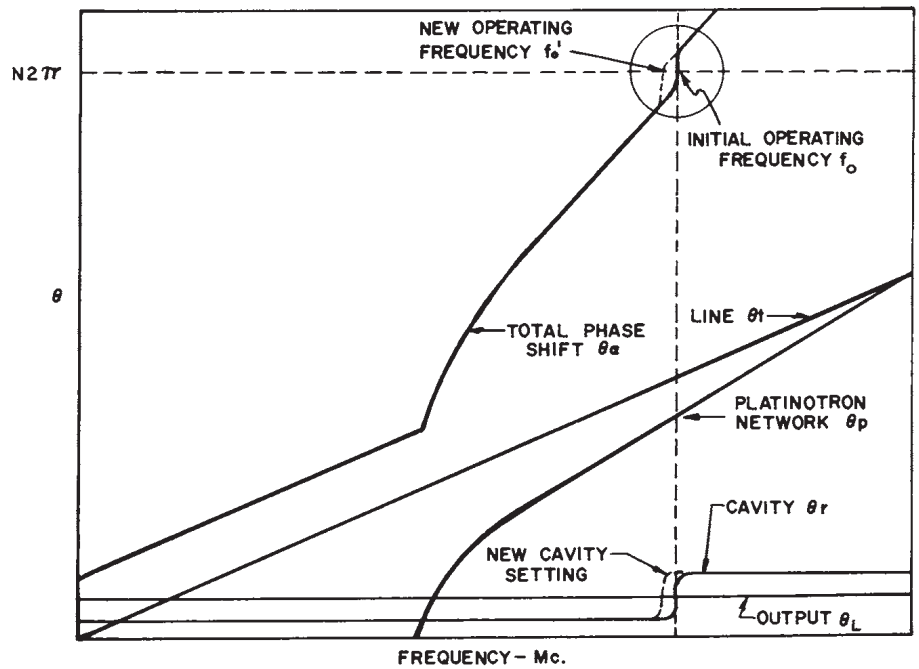

Fig. 31. Influence of cavity tuning on system frequency.

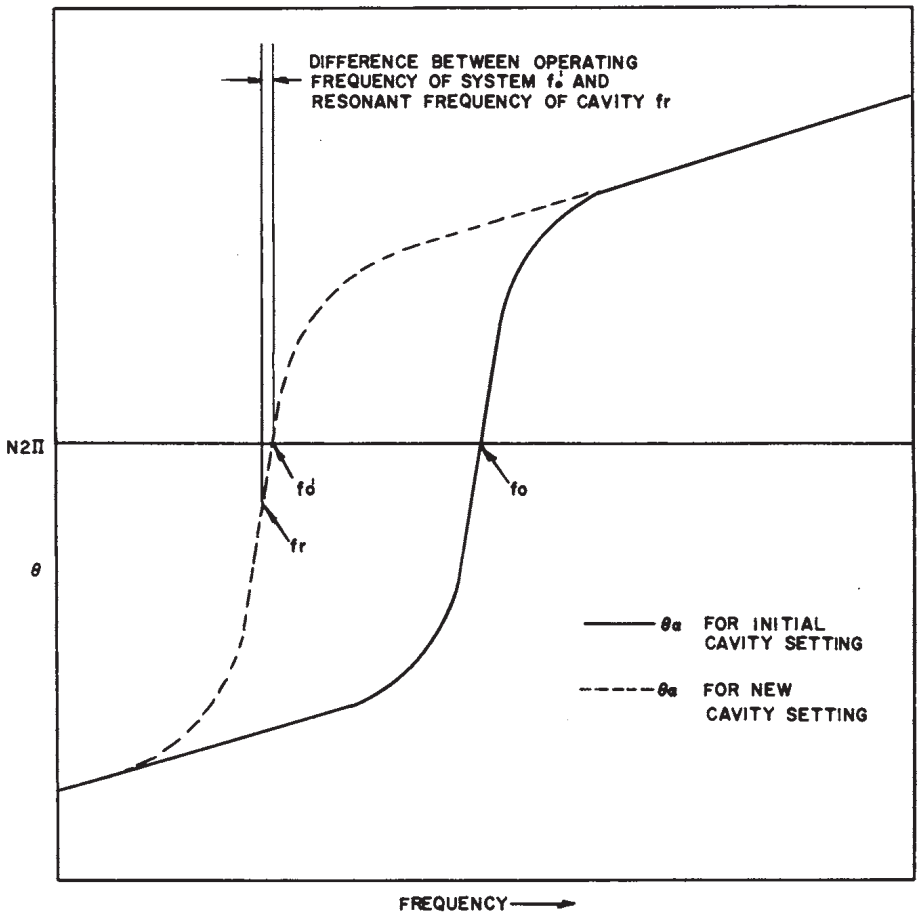

FIG. 32. Expansion of encircled area of Fig. 31. Difference between the system frequency and the resonant frequency of stabilizing cavity is indicated.

It is therefore desirable to place the operating frequency of the system close to the resonant frequency of the cavity. This can easily be done by appropriate adjustment in the length of the transmission line as shown in Fig. 33. Hence, by roughly ganging a line stretcher to the cavity, it is possible to obtain stabilization under optimum operating conditions over an appreciable tuning range. Without the line stretcher, tuning of the order of 0.5% can be obtained without undue degradation of system performance.

By the use of a combination tunable cavity and line stretcher, tuning might be carried on over a very wide frequency range if it were not for the fact that the platinotron is an electronically re-entrant device. The requirement of electron re-entrancy limits the tuning to bands of 180° phase shift about the complete platinotron network. For a platinotron

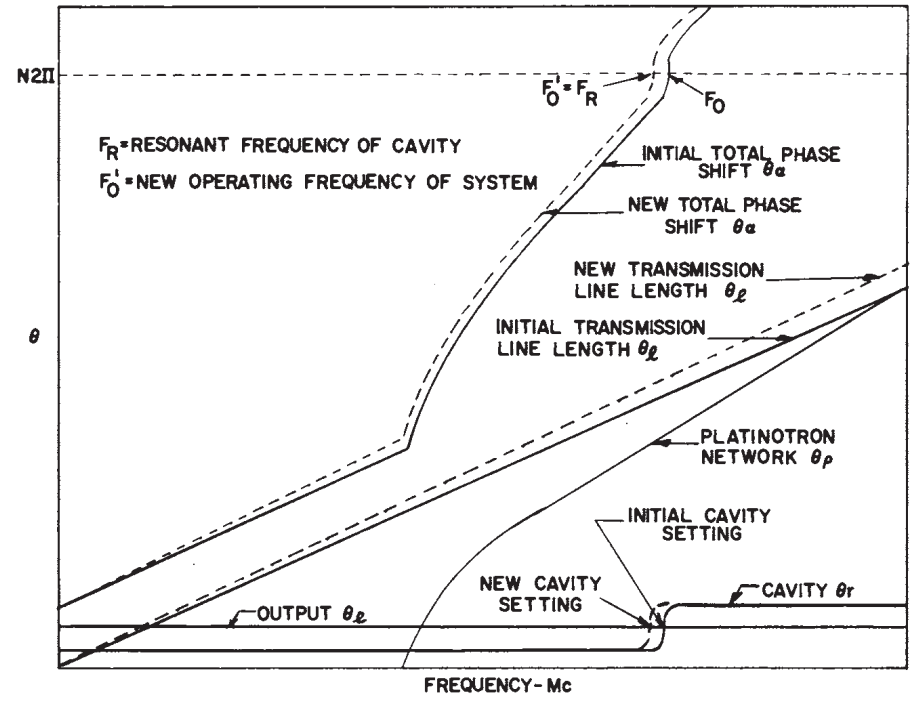

FIG. 33. Influence of combined use of line stretcher and cavity tuning to produce proper operation over wide frequency band.

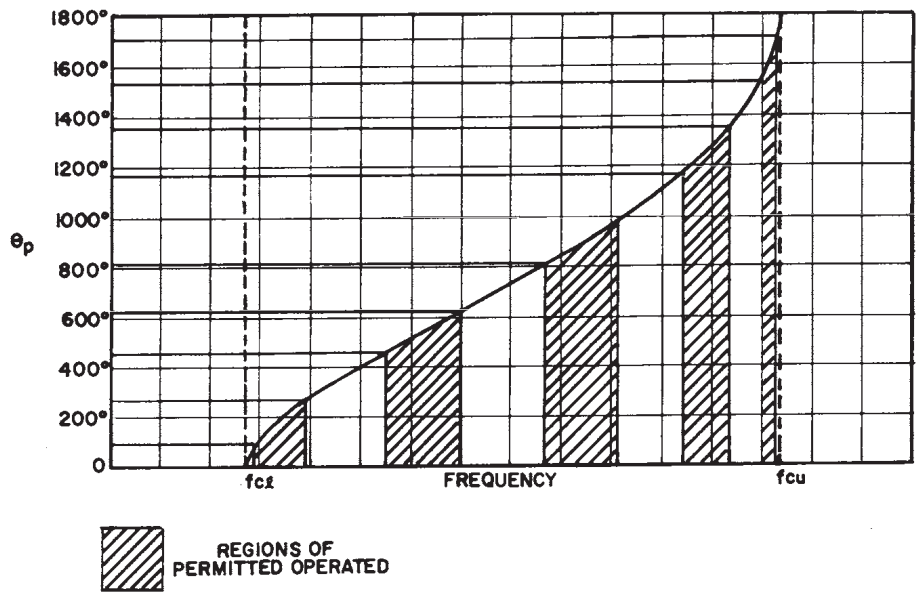

FIG. 34. Limitations on tuning range imposed by consideration of the re-entrance of the space charge in the interaction space.

network with ten network sections, this results in a set of bands within which tuning is possible, as illustrated in Fig. 34. If the difference between the lower cutoff frequency and the upper cutoff frequency of the platinotron networks is large, as it frequently is, respectable tuning ranges of the order of 6–10% are possible. If the separation between the upper and lower cutoff frequencies of the platinotron network is held constant, the frequency width of the 180° bands within which tuning is possible becomes smaller as the number of network sections increases.

It is the practice to design a tube to operate within only one of the several bands available because of both practical design and application considerations. It is also the practice to design in one of the two lower frequency bands because the characteristic impedance of the network is higher there, a condition which favors interaction between the network and the electron stream.

List of Symbols

θ_p	phase shift across the platinotron
P_o,rf	rf power output in kw
K	proportionality constant
P_i,rf	rf power input in kw
L_s	strap inductance
C_s	capacity between straps
Z_c	input impedance to loading sections of network
ω	angular frequency
ω_c	network lower cutoff angular frequency
Z_p	characteristic impedance of platinotron network
d	distance between vane tips
λ_s	wavelength along network as seen by electron beam
V	phase velocity
V_0	anode voltage at which electrons graze anode at synchronous velocity
m/e	mass to charge ratio of an electron
N	number of vanes
B	magnetic flux density (gauss)
B_0	value of magnetic field for grazing of anode by electrons at synchronous velocity
r_a	anode radius
r_c	cathode radius
θ	phase shift of each network section
t	time
t'	time for rotation of electron around anode
M	an integer
L_c	inductance of network cavity

ll' output reflection reference plane
rr' cavity terminals reference plane
Z_0 characteristic impedance
f_u unstabilized frequency
f_s stabilized frequency
$\Delta\theta$ incremental phase shift
θ_l phase shift of output reflection
θ_α total loop phase shift
$\Delta f_{\mu\pi}$ incremental frequency change in an unstabilized π mode magnetron
f frequency
f_0 unperturbed frequency
$S_{s/\mu\pi}$ improvement factor of Stabilotron over an unstabilized π mode magnetron
ΔI incremental current

References

1. Classified work sponsored by Bureau of Ships at Raytheon Company, 1948–1950.
2. R. R. WARNECKE, W. KLEEN, A. LERBS, O. DOEHLER, AND H. HUBER, The magnetron-type traveling-wave amplifier tube. *Proc. I.R.E.* (*Inst. Radio Engrs.*) **38**, 486–495 (1950).
3. Suitable expressions of Z_c for some common tube geometries are given by G. B. COLLINS, "Microwave Magnetrons," pp. 49–65. McGraw-Hill, New York, 1948.